Density Matrix Renormalization Group in Quantum Chemistry

Markus Reiher

Laboratorium für Physikalische Chemie, ETH Zürich, Switzerland

`http://www.reiher.ethz.ch`

June 2017

Four Lectures on DMRG in Quantum Chemistry

1. 'First-Generation' Density Matrix Renormalization Group (DMRG) in Quantum Chemistry
2. 'Second-Generation' DMRG:
   Matrix Product and Tensor Network States
   Matrix Product Operators
3. Some (of our) Results of Quantum-Chemical DMRG Calculations

Very useful introductory reference:

U. Schollwöck, *The density-matrix renormalization group in the age of matrix product states*, arXiv: 1008.3477v2

Reviews on DMRG in Quantum Chemistry

1. Ö Legeza, R. M. Noack, J. Sólyom and L. Tincani, Applications of Quantum Information in the Density-Matrix Renormalization Group, Lect. Notes Phys., 739,653-664 (2008)
2. G. K.-L. Chan, J. J. Dorando, D. Ghosh, J. Hachmann, E. Neuscamman, H. Wang, T. Yanai, An Introduction to the Density Matrix Renormalization Group Ansatz in Quantum Chemistry, Prog. Theor. Chem. and Phys., 18, 49 (2008)
3. D. Zgid and G. K.-L. Chan, The Density Matrix Renormalisation Group in Quantum Chemistry, Ann. Rep. Comp. Chem., 5, 149, (2009)
4. K. H. Marti, M. Reiher, The Density Matrix Renormalization Group Algorithm in Quantum Chemistry, Z. Phys. Chem., 224, 583-599 (2010)
5. G. K.-L. Chan and S. Sharma, The density matrix renormalization group in quantum chemistry, Ann. Rev. Phys. Chem., 62, 465 (2011)
6. K. H. Marti, M. Reiher, New Electron Correlation Theories for Transition Metal Chemistry, Phys. Chem. Chem. Phys., 13, 6750-6759 (2011)
7. Y. Kurashige, Multireference electron correlation methods with density matrix renormalisation group reference functions, Mol. Phys. 112, 1485-1494 (2014)
8. S. Wouters and D. Van Neck, The density matrix renormalization group for ab initio quantum chemistry, Eur. Phys. J. D 68, 272 (2014)
9. T. Yanai, Y. Kurashige, W. Mizukami, J. Chalupský, T. N. Lan, M. Saitow, Density matrix renormalization group for ab initio Calculations and associated dynamic correlation methods,Int. J. Quantum Chem. 115, 283-299 (2015)
10. S. Szalay, M. Pfeffer, V. Murg, G. Barcza, F. Verstraete, R. Schneider, Ö. Legeza, Tensor product methods and entanglement optimization for ab initio quantum chemistry, Int. J. Quantum Chem. 115, 1342 (2015)
11. G. Chan, A. Keselman, N. Nakatani, Z. Li, S. White, Matrix product operators, matrix product states, and ab initio density matrix renormalization group algorithms, J. Chem. Phys. 145, 014102 (2016)

Lecture 1

'First-Generation' DMRG in Quantum Chemistry

1. Standard Configuration Interaction in Explicit Second Quantization
2. Dimension Reduction by Decimation
3. Elements of the DMRG Algorithm

Non-Relativistic Many-Electron Hamiltonian

- many-electron Hamiltonian in position space (Hartree atomic units)

$$H_{el} = \sum_i^N \left(-\frac{1}{2}\nabla_i^2 - \sum_I \frac{Z_I}{r_{iI}} \right) + \sum_{i<j}^N \frac{1}{r_{ij}} \tag{1}$$

  with $r_{ij} = |\boldsymbol{r}_i - \boldsymbol{r}_j|$ and N being the number of electrons.

- eigenvalue equation: electronic Schrödinger equation

$$H_{el}\ \Psi_{el}^{\{\boldsymbol{R}_I\}}(\{\boldsymbol{r}_i\})\ =\ E_{el}(\{\boldsymbol{R}_I\})\ \Psi_{el}^{\{\boldsymbol{R}_I\}}(\{\boldsymbol{r}_i\}) \tag{2}$$

- central in electronic structure theory: how to approximate Ψ_{el} ?

Standard Procedure: Construction of Many-Electron Basis

- Construct many-electron (determinantal) basis set $\{\Phi_I\}$ from a given (finite) one-electron (orbital) basis set ϕ_i
- From the solution of the Roothaan–Hall equations, one obtains n orbitals from n one-electron basis functions.
- From the N orbitals with the lowest energy, the Hartree–Fock (HF) Slater determinant is constructed.
- The other determinants (configurations) are obtained by subsequent substitution of orbitals in the HF Slater determinant Φ_0:

$$\{\Phi_I\} \rightarrow \{\Phi_i^a\} \rightarrow \{\Phi_{ij}^{ab}\} \rightarrow \{\Phi_{ijk}^{abc}\} \tag{3}$$

- Determinants are classified by number of 'excitations' (= substitutions in HF reference determinant) into virtual orbitals.

Standard Full Configuration Interaction (FCI)

- The number of possible determinants is determined by the number of virtual orbitals $n - N$.
- Including all possible excited Slater determinants for a finite or infinite one-electron basis set leads to the so-called **full CI** approach.
- Number of Slater determinants n_{SD} for N spin orbitals chosen from a set of n spin orbitals (slang: N electrons in n spin orbitals):

$$n_{\mathrm{SD}} = \binom{n}{N} = \frac{n!}{N!(n-N)!} \tag{4}$$

Example: There are $\approx 10^{12}$ different possibilities to distribute 21 electrons in 43 spin orbitals.

- *In physics FCI is called exact diagonalization.*

Truncated CI Wave Functions

Standard recipe to avoid the factorial scaling of the many-electron basis-set size: **truncate basis**! *Note: basis is pre-defined!*

Assumption: Substitution hierarchy is a useful measure to generate a systematically improvable basis set.

CIS: all singly-(S)-excited determinants are included:

$$\Psi_{el}^{\mathrm{CIS}} = C_0\Phi_0 + \sum_{(ai)} C_{(ai)}\Phi_i^a \tag{5}$$

CISD: all singly- and doubly-(D)-excited determinants are included:

$$\Psi_{el}^{\mathrm{CISD}} = C_0\Phi_0 + \sum_{(ai)} C_{(ai)}\Phi_i^a + \sum_{(ai)(bj)} C_{(ai,bj)}\Phi_{ij}^{ab} \tag{6}$$

$$C_0, C_{(ai)}, C_{(ai,bj)} \in \{C_I\} \tag{7}$$

Determination of the CI Expansion Coefficients C_I

The CI expansion coefficients C_I determined by variational principle:

- write down the expectation value for the energy
- introduce the determinantal basis set
- vary the energy in order to minimize it

Expectation value for the CI electronic energy:

$$E_{el}^{\mathrm{CI}} = \frac{\left\langle \Psi_{el}^{\mathrm{CI}} \right| H_{el} \left| \Psi_{el}^{\mathrm{CI}} \right\rangle}{\left\langle \Psi_{el}^{\mathrm{CI}} \middle| \Psi_{el}^{\mathrm{CI}} \right\rangle} \tag{8}$$

Insert expansion of Slater determinants:

$$E_{el}^{\mathrm{CI}} = \frac{\sum_{K,L} C_K^* C_L \left\langle \Phi_K \right| H_{el} \left| \Phi_L \right\rangle}{\sum_{K,L} C_K^* C_L \left\langle \Phi_K \middle| \Phi_L \right\rangle} \tag{9}$$

The CI Eigenvalue Problem

Calculate all derivatives $\partial E_{el}^{\mathrm{CI}} \,/\, \partial C_K^*$ and set them equal to zero, which yields the **CI eigenvalue problem:**

$$\boldsymbol{H} \cdot \boldsymbol{C} = \boldsymbol{C} \cdot \boldsymbol{E}_{el} \tag{10}$$

Essential: $\boldsymbol{H}$ is constructed from matrix elements $\langle \Phi_K | \, H_{el} \, | \Phi_L \rangle$ in the pre-defined determinantal basis $\{\Phi_K\}$

By solving the CI eigenvalue problem, ground and excited electronic states of the system are obtained.

$\boldsymbol{E}_{el}$ is diagonal matrix with total energies of all electronic states that can be expressed in basis given (M determinants yield M electronic states).

Standard 'Technical' Trick: Second Quantization

Operators and wave functions are expressed in terms of creation and annihilation operators to implement the Slater–Condon rules for the evaluation of matrix elements $\langle \Phi_K | H_{el} | \Phi_L \rangle$ directly into the formalism.

H_{el} in second quantization (i, j, k, l are spin orbital indices):

$$\begin{aligned} \Rightarrow \qquad H_{el} &= \sum_{ij} \langle \phi_i | h(i) | \phi_j \rangle a_i^\dagger a_j \\ &+ \frac{1}{2} \sum_{ijkl} \langle \phi_i(1) \langle \phi_k(2) | g(1,2) | \phi_l(2) \rangle \phi_j(1) \rangle a_i^\dagger a_j^\dagger a_k a_l \end{aligned} \tag{11}$$

CI wave function in second quantization:

$$\Psi_{el}^{\mathrm{FCI}} = C_0 \Phi_0 + \sum_{(ai)} C_{(ai)} a_a^\dagger a_i \Phi_0 + \sum_{(ai)(bj)} C_{(ai,bj)} a_b^\dagger a_j a_a^\dagger a_i \Phi_0 \cdots \tag{12}$$

CI Energy in Second Quantization

$$E_{el}^{\mathrm{CI}} = \left\langle \Psi_{el}^{\mathrm{CI}} \middle| H_{el} \middle| \Psi_{el}^{\mathrm{CI}} \right\rangle \quad (13)$$

$$= \sum_{ij}^{n} \underbrace{\sum_{KL} C_K^* C_L t_{ij}^{KL}}_{\gamma_{ij}} \underbrace{\langle \phi_i(1) | h(1) | \phi_j(1) \rangle}_{\equiv h_{ij}}$$

$$+ \frac{1}{2} \sum_{ijkl}^{n} \underbrace{\sum_{KL} C_K^* C_L T_{ijkl}^{KL}}_{\Gamma_{ijkl}} \underbrace{\langle \phi_i(1) \langle \phi_k(2) | g(1,2) | \phi_l(2) \rangle \phi_j(1) \rangle}_{g_{ijkl}} \quad (14)$$

$$= \sum_{ij}^{n} \gamma_{ij} h_{ij} + \frac{1}{2} \sum_{ijkl}^{n} \Gamma_{ijkl} g_{ijkl} \quad (15)$$

t_{ij}^{KL} or T_{ijkl}^{KL} are matrix elements of determinantal basis functions over pairs or quadruples of elementary operators $a^\dagger$ and a.

γ_{ij} are Γ_{ijkl} are density matrix elements.

Is there a better way to construct the finite-dimensional determinantal basis set in order to avoid the factorial scaling?

Coupled-Cluster — An Advanced CI-type Wave Function

Ansatz:

$$\Psi_{\rm el}^{\rm CC} = \exp\left(T\right)\, \Phi_{\rm el}^{\rm HF} \tag{16}$$

Excitation operator:

$$T = T_1 + T_2 + T_3 + \cdots \tag{17}$$

where

$$T_\alpha = \sum_{\underbrace{ab\cdots}_{\alpha\ \text{times}}\underbrace{ij\cdots}_{\alpha\ \text{times}}} \overbrace{t_{ij\cdots}^{ab\cdots}}^{\text{cluster-amplitudes}} \underbrace{\cdots a_b^\dagger a_j a_a^\dagger a_i}_{\alpha\ \text{pairs}\ a^\dagger a} \quad \Rightarrow \quad T_1 = \sum_{ai} t_i^a a_a^\dagger a_i \tag{18}$$

Notation:

CCS $(T = T_1)$, CCSD $(T = T_1 + T_2)$, CCSDT $(T = T_1 + T_2 + T_3)$,$\cdots$

Coupled-cluster improves on truncated CI, because certain (disconnected) higher excited configurations (e.g., $t_i^a a_a^\dagger a_i t_{jk}^{bc} a_c^\dagger a_k a_b^\dagger a_j$) are included.

Is there a better way to construct the finite-dimensional determinantal basis set in order to avoid the factorial scaling?

Let's investigate FCI from a different perspective:

Many-Electron Hamiltonian in Second Quantization

- many-electron Hamiltonian in second quantization

$$H_{el} = \sum_{\substack{i,j\\\sigma}} h_{ij} a^\dagger_{i\sigma} a_{j\sigma} + \frac{1}{2} \sum_{\substack{i,j,k,l\\\sigma,\sigma'}} V_{ijkl} a^\dagger_{i\sigma} a^\dagger_{j\sigma'} a_{k\sigma'} a_{l\sigma} \tag{19}$$

  with $\sigma \in \{\alpha, \beta\}$ and the creators and annihilators $a_{i\sigma}$ and $a^\dagger_{i\sigma}$, resp.

- with one-electron integrals h_{ij}

$$h_{ij} = \int \phi_i^*(\boldsymbol{r}) \left(-\frac{1}{2}\nabla^2 - \sum_I \frac{Z_I}{r_I} \right) \phi_j(\boldsymbol{r})\, d^3r \tag{20}$$

- and two-electron integrals V_{ijkl}

$$V_{ijkl} = \int\int \frac{\phi_i^*(\boldsymbol{r}_1)\phi_j^*(\boldsymbol{r}_2)\phi_k(\boldsymbol{r}_2)\phi_l(\boldsymbol{r}_1)}{r_{12}}\, d^3r_1 d^3r_2 \tag{21}$$

  with spatial orbitals ϕ_i (i, j, k, l now spatial orbital indices).

Full CI in (Explicit) Second Quantization

- Elementary operators: $a^{\dagger}_{i\sigma}$ and $a_{i\sigma}$
- Hamiltonian matrix is now constructed from the matrix representation for the elementary operators by direct products
- **By contrast to standard procedure, instead of evaluating the action of the elementary operators on the determinantal basis functions, we set-up a matrix representation of the elementary operators and construct a matrix representation of the Hamiltonian DIRECTLY.**

  This Hamiltonian matrix can then be diagonalized.

Elementary operators in (Explicit) Second Quantization

- $a^\dagger_{i\sigma}$ and $a_{i\sigma}$ operate on spin orbital with two states: occ. and unocc.

$$|0\rangle_{i\sigma} = \begin{pmatrix} 1 \\ 0 \end{pmatrix} \text{ and } |1\rangle_{i\sigma} = \begin{pmatrix} 0 \\ 1 \end{pmatrix} \tag{22}$$

- Corresponding matrix representation of elementary operators:

$$a^\dagger_{i\sigma}|0\rangle_{i\sigma} = |1\rangle_{i\sigma} \quad \Longleftrightarrow \quad \begin{pmatrix} 0 & 0 \\ 1 & 0 \end{pmatrix} \begin{pmatrix} 1 \\ 0 \end{pmatrix} = \begin{pmatrix} 0 \\ 1 \end{pmatrix} \tag{23}$$

$$a^\dagger_{i\sigma}|1\rangle_{i\sigma} = 0 \quad \Longleftrightarrow \quad \begin{pmatrix} 0 & 0 \\ 1 & 0 \end{pmatrix} \begin{pmatrix} 0 \\ 1 \end{pmatrix} = \begin{pmatrix} 0 \\ 0 \end{pmatrix} \tag{24}$$

$$a_{i\sigma}|0\rangle_{i\sigma} = 0 \quad \Longleftrightarrow \quad \begin{pmatrix} 0 & 1 \\ 0 & 0 \end{pmatrix} \begin{pmatrix} 1 \\ 0 \end{pmatrix} = \begin{pmatrix} 0 \\ 0 \end{pmatrix} \tag{25}$$

$$a_{i\sigma}|1\rangle_{i\sigma} = |0\rangle_{i\sigma} \quad \Longleftrightarrow \quad \begin{pmatrix} 0 & 1 \\ 0 & 0 \end{pmatrix} \begin{pmatrix} 0 \\ 1 \end{pmatrix} = \begin{pmatrix} 1 \\ 0 \end{pmatrix} \tag{26}$$

Matrices for Hamiltonian in (Explicit) Second Quantization

- Dimension of elementary operators defined for orbital space of n spin orbitals with 2 states each: $2^n \Rightarrow$ dimension of the Hamiltonian is 2^n

  (NB: for spatial orbitals we have 4^n where 4 is the number of states per orbital [empty, up, down, doubly occupied])

- 2^n-dimensional elementary operator: (the spin index has been omitted for the sake of clarity)

$$a_i^\dagger = \underbrace{\begin{pmatrix} 1 & 0 \\ 0 & -1 \end{pmatrix}_1 \otimes \cdots \otimes \begin{pmatrix} 1 & 0 \\ 0 & -1 \end{pmatrix}_{i-1}}_{\substack{\text{matrix structure needed for anticommutation} \\ \text{cf. Jordan–Wigner transformation}}} \otimes \begin{pmatrix} 0 & 0 \\ 1 & 0 \end{pmatrix}_i \otimes \begin{pmatrix} 1 & 0 \\ 0 & 1 \end{pmatrix}_{i+1} \otimes \cdots \otimes \begin{pmatrix} 1 & 0 \\ 0 & 1 \end{pmatrix}_n$$

- Then, $2^n \times 2^n$-matrix of term of the one-electron part of Hamiltonian reads:

$$h_{ij} a_i^\dagger a_j =$$

$$h_{ij} \left[\begin{pmatrix} 1 & 0 \\ 0 & -1 \end{pmatrix}_1 \otimes \cdots \otimes \begin{pmatrix} 1 & 0 \\ 0 & -1 \end{pmatrix}_{i-1} \otimes \begin{pmatrix} 0 & 0 \\ 1 & 0 \end{pmatrix}_i \otimes \begin{pmatrix} 1 & 0 \\ 0 & 1 \end{pmatrix}_{i+1} \otimes \cdots \otimes \begin{pmatrix} 1 & 0 \\ 0 & 1 \end{pmatrix}_n \right]$$

$$\times \left[\begin{pmatrix} 1 & 0 \\ 0 & -1 \end{pmatrix}_1 \otimes \cdots \otimes \begin{pmatrix} 1 & 0 \\ 0 & -1 \end{pmatrix}_{j-1} \otimes \begin{pmatrix} 0 & 1 \\ 0 & 0 \end{pmatrix}_j \otimes \begin{pmatrix} 1 & 0 \\ 0 & 1 \end{pmatrix}_{j+1} \otimes \cdots \otimes \begin{pmatrix} 1 & 0 \\ 0 & 1 \end{pmatrix}_n \right]$$

- Similar expression for the two-electron part, but product of four 2^n-dimensional elementary matrices

Nothing has been gained yet!

Even worse: Huge matrices have been generated which contain mostly zeros and need to be multiplied and added.

Nothing has been gained yet!

Even worse: Huge matrices have been generated which contain mostly zeros and need to be multiplied and added.

Need to find a way to reduce the dimension !

What is the best reduced many-particle basis?

First attempt: Wilson's renormalization group

Wilson's Renormalization Group: Dimension Reduction

1. Choose a number of orbitals l whose many-electron Hamiltonian $H_{el}^{(l)}$ can still be constructed and exactly diagonalized.

2. Diagonalize $H_{el}^{(l)}$ of dimension 2^l (or 4^l for spatial orbitals) and select m lowest-energy eigenvectors out of the 2^l eigenvectors.

3. Reduce the dimension of $H_{el}^{(l)}$ from 2^l to m by transformation with the rectangular $m \times 2^l$ matrix of m eigenvectors of $H_{el}^{(l)}$.

4. Construct $H_{el}^{(l+1)}$ from $H_{el}^{(l)}$ and $H_{el}^{(1)}$ defined for an orbital taken from the $n - l$ remaining orbitals.

5. Continue with 2) until $l + 1 = n$.

Issues with Wilson's Renormalization Group

- $H_{el}^{(l)}$ requires exact diagonalization (or a subspace iteration technique like Lanczos, which produces a large portion of the low-energy eigenvectors) and thus its dimension 2^l is limited and l must therefore be rather small

- No guarantee that reduced basis is optimum choice in some sense.

- No information from those $n - l$ remaining orbitals, which have not been considered at the lth iteration step, is taken into account in the construction of $H_{el}^{(l)}$ (particularly bad, when l is small)

What is the best reduced many-particle basis in terms of a least-squares fit?

Second attempt: White's DMRG

— transform with eigenvectors of a reduced density matrix

S. R. White, *Phys. Rev. Lett.* **1992** *69* 2863; *Phys. Rev. B* **1993** *48* 10345

The (two-site) DMRG Algorithm: Terminology

- arrange all **spatial** orbitals as a one-dimensional lattice
- lattice consists of sites

$$\underbrace{\overbrace{\bullet}^{\text{site}} \; \bullet \; \bullet \; \bullet \; \cdots \; \bullet}_{\text{lattice}} \tag{27}$$

- the sites of solid state physics are the orbitals in quantum chemistry
- divide lattice into system block, two single sites, environment block

$$\boxed{\bullet \;\; \bullet \;\; \bullet \;\; \cdots \;\; \bullet} \qquad \bullet \qquad \bullet \qquad \boxed{\bullet \;\; \bullet \;\; \bullet \;\; \cdots \;\; \bullet}$$

system

(active subsystem)

(explicitly treated subsystem)

environment

(complementary subsystem)

- the joined systems (=CAS) are called the 'superblock'

The DMRG Algorithm: Initialization

- Construct many-particle states explicitly on active subsystem

→ actually: find matrix representation of elementary operators defined on this subsystem

- NB: For a total(!) system of N electrons, many-particle states with 0 to a maximum of N electrons need to be considered
- Hence, active subsystem can comprise only few orbitals (too many sites prohibitive because of factorial scaling of states)
- Find a way to increase the number of orbitals (blocking), while keeping the number of basis states on the active subsystem constant (decimation)

The DMRG Algorithm: Blocking

- enlarge the system (and environment) by one site ('blocking')

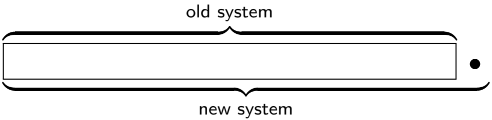

- new states are tensor products of those on old system + those on new site
- calculate operators of new system as direct product of operators defined for old system and new site
- Dimension of operators on old system: m; Dim. of ops. on single site: 4
  $\Rightarrow$ Dimension of operators defined on new system: $4m$

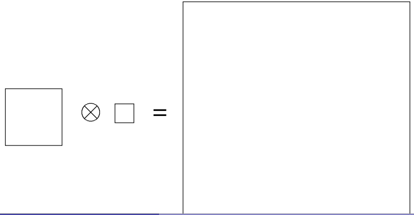

Construction & Diagonalization of Total Hamiltonian

- consider system and environment each enlarged by one of the explicitly treated sites (dimension for both: $4m$)
- any electronic state defined on the total orbital space (superblock) can be written as a tensor product over system $|i\rangle$ and environment $|j\rangle$ basis states

$$\Psi_{el}^{\mathrm{DMRG}} = \sum_{ij} \psi_{ij} \, |i\rangle \otimes |j\rangle \tag{28}$$

- corresponding superblock Hamiltonian $H_{\text{superblock}}$ is calculated as a sum of all elementary operator products defined on enlarged system and enlarged environment (dimension: $4m \times 4m = 16m^2$)
- NB: realize that in the first set of iterations (sweep), in which the active subsystem grows orbital by orbital, guessing of a reduced number of states on the environment is required (warm-up)
- diagonalize $H_{\text{superblock}}$ to obtain CI-type coefficients ψ_{ij} (scaling: $(16m^2)^3 \approx m^6$ for large m → subspace methods: Davidson's diagonalizer)

Construction & Diagonalization of Reduced Density Matrix

- The DMRG CI-type coefficients ψ_{ij} carry two indices as they are explicitly obtained for the i-th system and the j-th environment basis state.
- The reduced density matrix $\rho^{s/e}$ (RDM) for the system can be obtained by tracing out all (sub)states j from the environment:

$$\rho^{s/e}_{ii'} = \sum_{j \in \{e\}} \psi_{ij}\psi_{i'j} \tag{29}$$

- This matrix $\rho^{s/e}_{ii'}$ is of dimension $4m$
- m eigenvectors of $\rho^{s/e}$ can be used for the dimension reduction of all elementary operators from $4m$ back to the original dimension m

Understanding Relation of RDM to Least-Squares Fitting

- We have the following bases at our disposal:
  system: $\{|i\rangle; i = 1, \ldots, m_s\}$
  environment: $\{|j\rangle; j = 1, \ldots, m_e\}$
- In the product basis (bipartition) we express a pure state of the superblock (total system; real coefficients assumed):

$$\Psi_{el} = \sum_{ij} \psi_{ij} |i\rangle \otimes |j\rangle \tag{30}$$

- Now search for $m < m_s$ orthogonal, linear-independent system states $\{|u\rangle; u = 1, \ldots, m\}$
  into which we expand the approximate state

$$\widetilde{\Psi}'_{el} = \sum_{uj} c_{uj} |u\rangle \otimes |j\rangle \tag{31}$$

RDM, SVD, and Least-Squares Fitting

- We wish $\Psi_{el} \approx \widetilde{\Psi}'_{el}$ by requiring that

$$S' = \left|\Psi_{el} - \widetilde{\Psi}'_{el}\right|^2 = \text{ min} \tag{32}$$

- Introduce a similar reduced-dimensional basis on the environment: $\{|v\rangle; v = 1, \dots, m\}$ with $\langle j|v\rangle = c_{vj}$ and $\sum_j |c_{vj}|^2 = 1$ such that the approximate state takes the simple form

$$\widetilde{\Psi}_{el} = \sum_k c_k |u_k\rangle \otimes |v_k\rangle \tag{33}$$

(Schmidt decomposition)

- With $U_{ik} = \langle i|u_k\rangle$ and $V_{jk} = \langle j|v_k\rangle$ we have for the squared norm

$$S = \sum_{ij} \left[\psi_{ij} - \sum_k c_k U_{ik} V_{jk}\right]^2 \tag{34}$$

RDM, SVD, and Least-Squares Fitting

- **Here, we recognize the similarity to the least-squares fitting problem in linear algebra!**
- Hence, we may use singular value decomposition (SVD) of a rectangular matrix to minimize S → factorize $\psi = (\psi_{ij})$:

$$\psi = U \cdot D \cdot V^T \tag{35}$$

- The matrix $U = (U_{ik})$ is orthogonal and of dimension $m_s \times m_s$.
- The matrix $V = (V_{jk})$ is column-orthogonal and of dimension $m_e \times m_s$.
- D is an m_s-dimensional diagonal matrix and contains the singular values of ψ (assume $m_s \leq m_e$, otherwise consider ψ^T).

RDM, SVD, and Least-Squares Fitting

- The m largest diagonal elements of D are the desired coefficients c_k and the corresponding column vectors of U and V are the desired $|u_k\rangle$ and $|v_k\rangle$.
- **But how can one make the connection to the RDM?**
- Consider the von Neumann density operator for the superblock

$$\hat{\rho} = |\Psi_{el}\rangle\langle\Psi_{el}| \overset{(30)}{=} \sum_{ii'jj'} \psi_{ij}\psi_{i'j'}|i\rangle\langle i'| \otimes |j\rangle\langle j'| \tag{36}$$

- reduced density operator from tracing out the enviroment states

$$\hat{\rho}_s = Tr_e\hat{\rho} = \sum_{j''}\sum_{ii'jj'} \psi_{ij}\psi_{i'j'}|i\rangle\langle i'|\langle j''|j\rangle\langle j'|j''\rangle \tag{37}$$

$$= \sum_{ii'j} \psi_{ij}\psi_{i'j}|i\rangle\langle i'| \tag{38}$$

RDM, SVD, and Least-Squares Fitting

- The RDM is then obtained as

$$\rho_s = \psi \cdot \psi^T \quad \text{with} \quad (\rho_s)_{ii'} = \sum_j \psi_{ij}\psi_{i'j} \tag{39}$$

- for which we can insert the SVD

$$\rho_s = \psi \cdot \psi^T \overset{(35)}{=} (UDV^T) \cdot (VDU^T) = U \cdot D^2 \cdot U^T \tag{40}$$

- Hence, U diagonalizes ρ_s and thus its eigenvalues D_{ii}^2 are related to the coefficients c_k of the Schmidt decomposition !
- Thus, instead of calculating the SVD, one can diagonalize ρ_s to obtain the $c_k = \sqrt{D_{kk}^2}$ from the m highest eigenvalues of D^2 and the corresponding eigenvectors $|u_k\rangle$.
- I.e., the larger the eigenvalue D_{ii}^2, the better represents $|u_i\rangle$ the system part of the superblock state

RDM, SVD, and Least-Squares Fitting

- Accuracy of approximation can be measured by the truncation error ϵ

$$\epsilon = 1 - \sum_{k=1}^{m} D_{kk}^2 \tag{41}$$

Ö. Legeza, J. Röder, B. A. Hess, Phys. Rev. B 67 (2003) 125114

- This transfers to the accuracy of an observable O as follows

$$\begin{aligned}
|\langle O\rangle_{\Psi_{el}} - \langle O\rangle_{\widetilde{\Psi}_{el}}| &= |Tr(O\rho_s) - Tr(O\widetilde{\rho}_s)| = \left|\sum_{i=m+1}^{m_s} O_{ii} D_{ii}^2\right| \\
&\leq \sum_{i=m+1}^{m_s} |O_{ii}| D_{ii}^2 \leq \max_{i>m} |O_{ii}| \sum_{i=m+1}^{m_s} D_{ii}^2 \\
&= \max_{i>m} |O_{ii}| \epsilon
\end{aligned} \tag{42}$$

J. Röder, PhD Thesis, University of Erlangen, 2003

Pictorially: Diagonalization of the RDM

- reduced density matrix is diagonalized → $4m$ eigenpairs

$$U = \boxed{4m \times 4m}$$

Pictorially: Diagonalization of the RDM

- reduced density matrix is diagonalized → $4m$ eigenpairs

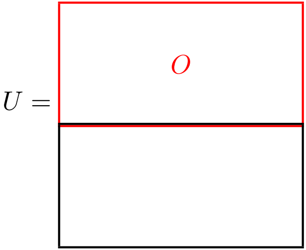

- choose the m eigenvectors with the highest eigenvalues

- keep m variable to always adjust to the optimum number of relevant eigenvectors (Ö. Legeza: dynamic block-state selection DBSS)

- selected eigenvectors transform the many-particle basis of the (enlarged) system to a reduced basis

Pictorially: Renormalization of Operators

- transformation by selected eigenvectors yields new many-particle basis of the system (optimum reduced m-dimensional basis in a least-squares sense)

- operators are now transformed to the new basis, i.e. renormalized:

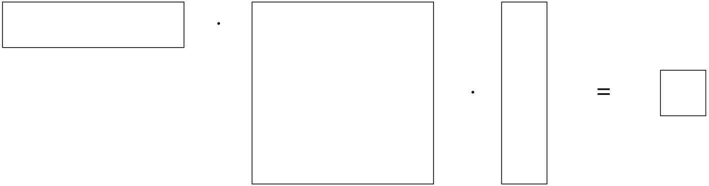

$$O^T \; \tilde{a}_{\text{new}} \; O \;=\; a_{\text{new}} \tag{43}$$

- columns of the transformation matrix O consist of the selected eigenvectors

- dimension of the operators is reduced from $4m$ to m

Features of the DMRG Algorithm

- DMRG is a CAS approach!
- DMRG iterations increase AS orbital by orbital until the environment is completely absorbed into the system.
- Then, the iteration direction is reversed to optimize the environment representation.
- This defines a 'linear' algorithm, and explains why the orbital ordering can be important (convergence to local minima possible!).

  G. Moritz, B. A. Hess, M. Reiher, *J. Chem. Phys.* **2005** *122* 024107
- It was thought that DMRG is therefore only beneficial for pseudo-one-dimensional molecules.
- DMRG state is a superposition of FCI-type basis states.
- An FCI/CAS solution can be converged; but the basis cannot be completely known in terms of CSFs if DMRG shall be efficient

DMRG Convergence for Complicated Electronic Structures

- If DMRG calculations shall be competitive, these issues must be addressed:
  - **dynamic correlation effects need to be included**
    see work of G. K.-L. Chan *et al.*, T. Yanai & Y. Kurashige *et al.* on multi-reference perturbation theory; problem: requires up to 4-body reduced density matrices! (see also last lecture)
  - **efficient warm-up sweep (environment guess)**
    see work of Ö. Legeza *et al.* (CI-DEAS and entanglement measures for orbital ordering)
  - **number of renormalized states m should be as small as possible**
- orbital ordering:
  crucial to avoid convergence to local energy minima in case of small m (especially, if no RDM noise or perturbation are considered)

  G. Moritz, B. A. Hess, M. Reiher, *J. Chem. Phys.* **2005** *122* 024107
- environment states: in principle, the better the approximation of environment states the faster convergence should be

  G. Moritz, M. Reiher, *J. Chem. Phys.* **2006** *124* 034103

Determining Factors of DMRG Convergence

1. (Choice of the one-electron basis set for the representation of the molecular orbitals)
2. Size of the active space (CAS)
3. Choice of the type of molecular orbitals (HF, NO's, localized orbitals, ..., DMRG-SCF)
4. Environment-state guess in the first sweep (CI-DEAS by Ö. Legeza or noise/perturbation added to RDM)
5. Ordering of orbitals (exploit entanglement measures, see below)
6. Number of renormalized subsystem states m ($=$ bond dimension, see later); extrapolate (run at least 3 calcs with varying m)

⇒ **All of these parameters must be reported for DMRG results !**

S. Keller, M. Reiher, Chimia 68 **2014** 200-203 [arXiv: 1401.5497]

Lecture 2

'Second-Generation' DMRG:
Matrix Product and Tensor Network States

1. New Parametrization of the Electronic Wave Function: Tensor Network States (TNS)
2. Matrix Product States (MPSs) and Matrix Product Operators (MPOs)

How to Efficiently Represent (Electronic) Quantum States?

- Tensor-product construction of the N-particle Hilbert space from 1-particle Hilbert spaces

$$\Psi_{el} = \sum_{i_1 i_2 \cdots i_n} C_{i_1 i_2 \cdots i_n} \; |i_1\rangle \otimes |i_2\rangle \otimes \cdots \otimes |i_n\rangle \tag{44}$$

- Dimension inreases exponentially with system size (4^n for spatial orbitals). $C_{i_1 i_2 \cdots i_n}$ ($=C_I$) is element of the coefficient tensor
- In principle, it should be sufficient to parameterize a manifold of states such that there exists a large overlap with the exact state.

F. Verstraete, *Adv. Phys.* **2008** *57* 143; quantum chemistry has always relied on this!

- How to reduce the complexity of Ψ_{el} by a class of variational wave functions that capture the physics of the Hamiltonian?

Parameterization of the Wave Function

$$\Psi_{el} = \sum_{i_1 i_2 \cdots i_L} C_{i_1 i_2 \cdots i_n} |i_1\rangle \otimes |i_2\rangle \otimes \cdots \otimes |i_n\rangle \tag{45}$$

- Configuration Interaction ansatz

$$|\mathrm{CI}\rangle = \left(1 + \sum_{\mu} C_{\mu} \hat{\tau}_{\mu}\right) |\mathrm{HF}\rangle \tag{46}$$

- Coupled Cluster ansatz

$$|\mathrm{CC}\rangle = \left(\prod_{\mu} [1 + t_{\mu} \hat{\tau}_{\mu}]\right) |\mathrm{HF}\rangle \tag{47}$$

- Restricted sum over basis states with a certain substitution pattern generated by 'excitation' operator $\hat{\tau}_{\mu}$
  → yields a pre-defined (!) many-particle basis set
- numerous specialized selection/restriction protocols

Instead of standard CI-type calculations by diagonalization/projection

$$\Psi_{el} = \sum_{i_1 i_2 \cdots i_n} C_{i_1 i_2 \cdots i_n} \, |i_1\rangle \otimes |i_2\rangle \otimes \cdots \otimes |i_n\rangle \tag{48}$$

construct CI coefficients from correlations among orbitals

$$\Psi_{el} = \sum_{i_1 i_2 \cdots i_n} C_{i_1 i_2 \cdots i_n} \, |i_1\rangle \otimes |i_2\rangle \otimes \cdots \otimes |i_n\rangle \tag{49}$$

$\Longrightarrow$ tensor construction of expansion coefficients

Some Early Tensor Network (TN) Approaches

... for spin Hamiltonians developed:

- 1-dimensional TN: **Matrix Product States** (MPS) / DMRG

  S. R. White, *Phys. Rev. Lett.* **1992** *69* 2863

  S. Römmer, S. Ostlund, *Phys. Rev. Lett.* **1995** *75* 3537

- 2-dimensional TN: **Projected Entangled Pair States** (PEPS)

  F. Verstraete, M. M. Wolf, D. Perez-Garcia, J. I. Cirac *PRL* **2006** *96* 220601

- higher-dimensional TN:
  Multiscale Entanglement Renormalization Ansatz (MERA)

  M. Aguado, G. Vidal, *Phys. Chem. Rev.* **2008** *100* 070404

MPS & DMRG

- Structure of White's DMRG wave function: Matrix Product States (MPS)

  S. Römmer, S. Ostlund, *Phys. Rev. Lett.* **1995** *75* 3537

$$\Psi_{el}^{\mathrm{MPS}} = \sum_{i_1 i_2 \cdots i_n} \left[A^{[i_1]} \cdots A^{[i_n]} \right] |i_1 \otimes i_2 \otimes \cdots \otimes i_n\rangle \tag{50}$$

- **DMRG algorithm defines a protocol for the iterative improvement of the matrices A^{i_j} by using the reduced density matrix (RDM) for the AS of the total system.**
- Transformation matrices $A^{[i]}$ represent the change of the many-electron basis when adding to the *active subsystem* (AS) states on a single orbital taken from the *environment*.
- In the finite-CAS DMRG, the first and last matrices $A^{[i_1]}$ and $A^{[i_n]}$, resp., are actually vectors (of length 4 for spatial orbitals).

Reconstruction of CI coefficients

- Reconstruct a CI-type wave function from the DMRG state, because
  - allows us to interpret/understand the states in the standard way,
  - makes DMRG calculations for different m values comparable,
  - allows us to study DMRG convergence in terms of determinants being picked up.

- MPS structure yields the CI coefficients:

$$\begin{aligned} C_{\{\mathbf{n}\}} \quad &= \quad \sum_{m}^{m_s} \sum_{m'}^{m_e} \psi_{m n_{l+1} n_{l+2} m'} \left(A_l^{[n_l]} \dots A_2^{[n_2]} \right)_{m;n_1} \\ & \quad \times \left(A_{l+3}^{[n_{l+3}]} \dots A_{n-1}^{[n_{n-1}]} \right)_{m';n_n} \end{aligned} \tag{51}$$

CI coefficient calculated from renormalization matrices and DMRG-state expansion coefficients $\psi_{m n_{l+1} n_{l+2} m'}$ (for active system of size l)

G. Moritz, M. Reiher, *J. Chem. Phys.* *126* **2007** 244109

Example: Transition Structure of Ozone

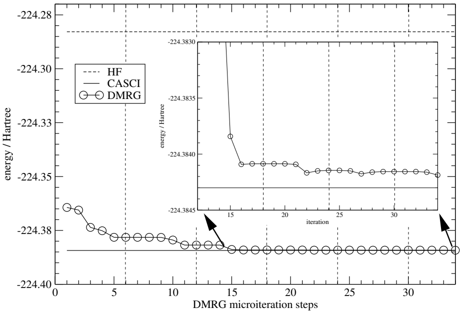
O_3 transition state energy

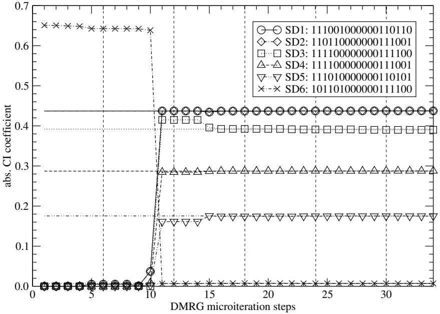
O_3 transition state CI coefficients

G. Moritz, M. Reiher, *J. Chem. Phys. 126* (2007) 244109

(see this reference also for a DMRG flow chart)

Example: Transition Structure of Ozone

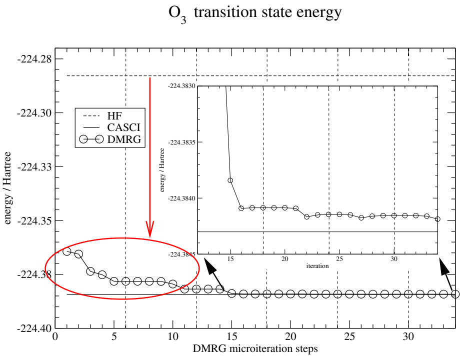

O_3 transition state energy

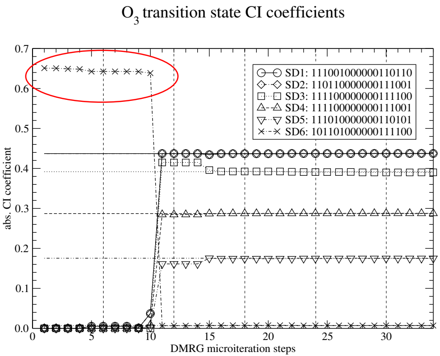

O_3 transition state CI coefficients

G. Moritz, M. Reiher, *J. Chem. Phys. 126* (2007) 244109

(see this reference also for a DMRG flow chart)

Example: Transition Structure of Ozone

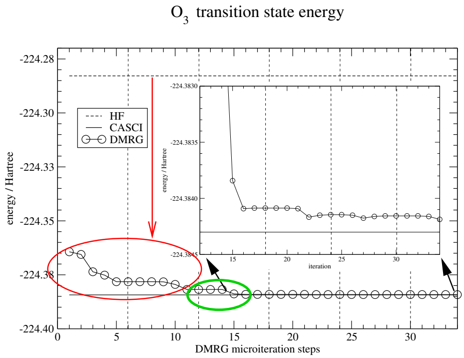
O_3 transition state energy

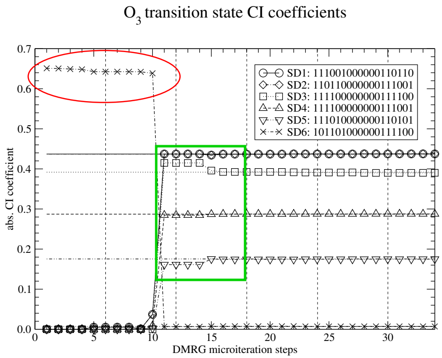
O_3 transition state CI coefficients

G. Moritz, M. Reiher, *J. Chem. Phys.* *126* (2007) 244109

(see this reference also for a DMRG flow chart)

SR-CAS Approach

- Our 2007 scheme could only reconstruct FCI from DMRG wave functions for which a FCI calculation was also possible.

- Cure: Sampling-Reconstruction Complete-Active-Space algorithm:

  Monte Carlo scheme for sampling configurations

- Only the most important configurations are kept.
- The accuracy is easily controlled by a completeness measure COM:

$$\mathrm{COM} = 1 - \sum_{I \in \{\mathrm{sample}\}} C_I^2 \tag{52}$$

K. Boguslawski, K. H. Marti, M. Reiher, *J. Chem. Phys. 134* (2011) 224101

Derivation of MPS Structure of DMRG Wave Function

The CI coefficient tensor $C_{i_1 i_2 \cdots i_n}$

$$\begin{aligned} \Psi_{el} &= \sum_{i_1 i_2 \cdots i_n} C_{i_1 i_2 \cdots i_n} \, |i_1\rangle \otimes |i_2\rangle \otimes \cdots \otimes |i_n\rangle \\ &\equiv \sum_{i_1 i_2 \cdots i_n} C_{i_1 i_2 \cdots i_n} \, |i_1, i_2, \ldots i_n\rangle \equiv \sum_I C_I \Phi_I \end{aligned} \tag{53}$$

can be decomposed by sequential SVDs, which clarifies the MPS structure of the DMRG wave function.

Consider a DMRG state function with the first orbital (from the left) in the AS and $(n-1)$ orbitals in the environment,

$$\Psi_{el}^{\text{DMRG}} = \sum_{i_1, \mathbf{j}} \psi_{i_1 \mathbf{j}} \, |i_1\rangle \otimes |\mathbf{j}\rangle \quad \text{with} \quad \mathbf{j} = (i_2 \ldots i_n) \tag{54}$$

Hence, the coefficient tensor $C_{i_1 i_2 \cdots i_n}$ is approximated by a matrix $\psi_{i_1 \mathbf{j}}$.

Derivation of MPS Structure of DMRG Wave Function

$\psi_{i_1\mathbf{j}}$ is of dimension $(m \times m^{n-1})$ and can be subjected to an SVD

$$\begin{aligned} C_{i_1 i_2 \cdots i_n} \;\rightarrow\; \psi_{i_1\mathbf{j}} = \psi_{i_1(i_2\ldots i_n)} \;&=\; \sum_{a_1}^{r_1} U_{i_1 a_1}\; D_{a_1 a_1}\; V^T_{a_1(i_2\ldots i_n)} \\ &\equiv\; \sum_{a_1}^{r_1} U_{i_1 a_1}\; C_{a_1 i_2\ldots i_n} \qquad (55) \end{aligned}$$

with the rank $r_1 \leq m$. Now, change notation:

a) matrix U is written as a collection of row vectors A^{i_1} with entries $A^{i_1}_{a_1} = U_{i_1 a_1}$.

b) coefficient tensor $C_{a_1 i_2\ldots i_n}$ is re-ordered as a matrix $\psi_{(a_1 i_2)(i_3\ldots i_n)}$ of dimension $(r_1 \cdot m \times m^{n-2})$

Derivation of MPS Structure of DMRG Wave Function

... so that we obtain for the original coefficient tensor

$$C_{i_1 i_2 \cdots i_n} = \sum_{a_1}^{r_1} A_{a_1}^{i_1} \; \psi_{(a_1 i_2)(i_3 \ldots i_n)} \tag{56}$$

Next, the matrix $\psi_{(a_1 i_2)(i_3 \ldots i_n)}$ is subjected to another SVD

$$\begin{aligned} \psi_{(a_1 i_2)(i_3 \ldots i_n)} &= \sum_{a_2}^{r_2} U_{(a1 i_2) a_2} \; D_{a_2 a_2} \; V^T_{a_2 (i_3 \ldots i_n)} && (57) \\ &\equiv \sum_{a_2}^{r_2} U_{(a_1 i_2) a_2} \; C_{a_2 i_3 \ldots i_n} && (58) \\ &\equiv \sum_{a_2}^{r_2} A_{a_1 a_2}^{i_2} \; \psi_{(a_2 i_3)(i_4 \ldots i_n)} && (59) \end{aligned}$$

where the last step is again just a change of notation ...

Derivation of MPS Structure of DMRG Wave Function

... which, however, allows us to write the original tensor in compact form

$$C_{i_1 i_2 \cdots i_n} = \sum_{a_1}^{r_1} \sum_{a_2}^{r_2} A^{i_1}_{a_1} A^{i_2}_{a_1 a_2} \ \psi_{(a_2 i_3)(i_4 \ldots i_n)} \tag{60}$$

Now, the new matrix $\psi_{(a_2 i_3)(i_4 \ldots i_n)}$ of dimension $(r_2 \cdot m \times m^{n-3})$ is subjected to the next SVD.

This 'game' continues until we finally obtain

$$\begin{aligned} C_{i_1 i_2 \cdots i_n} &= \sum_{a_1 \ldots a_n} A^{i_1}_{a_1} A^{i_2}_{a_1 a_2} \ldots A^{i_{n-1}}_{a_{n-2} a_{n-1}} A^{i_n}_{a_{n-1}} && (61) \\ &= A^{i_1} A^{i_2} \cdots A^{i_{n-1}} A^{i_n} && (62) \end{aligned}$$

where the sums are interpreted as matrix multiplications in the last step.

MPS Structure of Operators: MPOs

Consider occupation-number-vector basis states $|\boldsymbol{\sigma}\rangle$ and $|\boldsymbol{\sigma'}\rangle$.

The coefficients $w_{\boldsymbol{\sigma}\boldsymbol{\sigma'}}$ of a general operator

$$\widehat{\mathcal{W}} = \sum_{\boldsymbol{\sigma},\boldsymbol{\sigma'}} w_{\boldsymbol{\sigma}\boldsymbol{\sigma'}} |\boldsymbol{\sigma}\rangle\langle\boldsymbol{\sigma'}|, \tag{63}$$

may be encoded in matrix-product form

$$w_{\boldsymbol{\sigma},\boldsymbol{\sigma'}} = \sum_{i_1,\ldots,i_{n-1}} W_{1i_1}^{\sigma_1\sigma_1'} \cdots W_{i_{l-1}i_l}^{\sigma_l\sigma_l'} \cdots W_{i_{n-1}1}^{\sigma_n\sigma_n'}. \tag{64}$$

Combining Eqs. (63) and (64), operator $\widehat{\mathcal{W}}$ reads

$$\widehat{\mathcal{W}} = \sum_{\boldsymbol{\sigma}\boldsymbol{\sigma'}} \sum_{i_1,\ldots,i_{n-1}} W_{1i_1}^{\sigma_1\sigma_1'} \cdots W_{i_{l-1}i_l}^{\sigma_l\sigma_l'} \cdots W_{i_{n-1}1}^{\sigma_n\sigma_n'} \, |\boldsymbol{\sigma}\rangle\langle\boldsymbol{\sigma'}|. \tag{65}$$

Simplify Eq. (65) by contraction over the local site indices σ_l, σ_l' in $\boldsymbol{\sigma}, \boldsymbol{\sigma'}$:

$$\widehat{W}^l_{i_{l-1}i_l} = \sum_{\sigma_l, \sigma_l'} W^{\sigma_l \sigma_l'}_{i_{l-1}i_l} |\sigma_l\rangle\langle\sigma_l'|, \tag{66}$$

so that Eq. (65) reads

$$\widehat{\mathcal{W}} = \sum_{i_1,\ldots,i_{n-1}} \widehat{W}^1_{1i_1} \cdots \widehat{W}^l_{i_{l-1}i_l} \cdots \widehat{W}^n_{i_{n-1}1}. \tag{67}$$

Motivation for this: Entries of the resulting $\widehat{W}^l_{i_{l-1}i_l}$ matrices are the elementary operators $\hat{a}^\dagger_{l\sigma}$ and $\hat{a}_{l\sigma}$ acting on a single site (=orbital)!

In this way, the local-site MPS concept, which denotes for site l the l-th optimization step in a sweep, is transfered to operators (MPOs).

Why write a new code? – Two variants of DMRG:

Traditional DMRG

- $|\psi\rangle = \sum_{LR} C_{LR} |\boldsymbol{\sigma}_L\rangle \otimes |\boldsymbol{\sigma}_R\rangle$
- coefficients valid for one bipartition into L and R (need basis transformations)
- considered to be faster for ground state

MPO-DMRG

- $|\psi\rangle = \sum_{\boldsymbol{\sigma}} M^{\sigma_1} M^{\sigma_2} \cdots M^{\sigma_n} |\boldsymbol{\sigma}\rangle$
- coefficients valid for whole system
- Easy and efficient implementation of observables
- (NB: Both variants will perform similarly if implemented properly)

DMRG with Matrix Product States (MPS) and Matrix Product Operators (MPO)

Our new MPO-based DMRG program: QCMaquis

Download: http://www.reiher.ethz.ch/software/maquis.html

$$|\Psi\rangle = \sum_{\boldsymbol{\sigma}} c_{\boldsymbol{\sigma}} |\boldsymbol{\sigma}\rangle \quad \rightarrow \quad |\Psi\rangle = \sum_{\boldsymbol{\sigma}} \sum_{a_1,\ldots,a_{n-1}} M^{\sigma_1}_{1a_1} M^{\sigma_2}_{a_1a_2} \cdots M^{\sigma_n}_{a_{n-1}1} |\boldsymbol{\sigma}\rangle$$

$$\widehat{\mathcal{W}} = \sum_{\boldsymbol{\sigma},\boldsymbol{\sigma'}} w_{\boldsymbol{\sigma}\boldsymbol{\sigma'}} |\boldsymbol{\sigma}\rangle\langle\boldsymbol{\sigma'}| \quad \rightarrow$$

$$\widehat{\mathcal{W}} = \sum_{\boldsymbol{\sigma}\boldsymbol{\sigma'}} \sum_{b_1,\ldots,b_{n-1}} W^{\sigma_1\sigma'_1}_{1b_1} \cdots W^{\sigma_l\sigma'_l}_{b_{l-1}b_l} \cdots W^{\sigma_n\sigma'_n}_{b_{n-1}1} |\boldsymbol{\sigma}\rangle\langle\boldsymbol{\sigma'}|$$

S. Keller, M. Dolfi, M. Troyer, M. Reiher, J. Chem. Phys. 143, 244118 (2015)

MPS-MPO Operations: Expectation Values

$$\langle\phi|\widehat{\mathcal{W}}|\psi\rangle = \sum_{\substack{\sigma_L\sigma'_L\\ a_{L-1}a'_{L-1}b_{L-1}}} N^{\sigma_L\dagger}_{1a_{L-1}} W^{\sigma_L\sigma'_L}_{b_{L-1}1}\left(\cdots \sum_{\substack{\sigma_2\sigma'_2\\ a_1a'_1b_1}} N^{\sigma_2\dagger}_{a_2a_1} W^{\sigma_2\sigma'_2}_{b_1b_2}\right.$$

$$\left. \cdot \underbrace{\left(\sum_{\sigma_1\sigma'_1} N^{\sigma_1\dagger}_{a_11} W^{\sigma_1\sigma'_1}_{1b_1} M^{\sigma'_1}_{1a'_1}\right)} M^{\sigma'_2}_{a'_1a'_2}\cdots\right) M^{\sigma'_L}_{a'_{L-1}1}$$

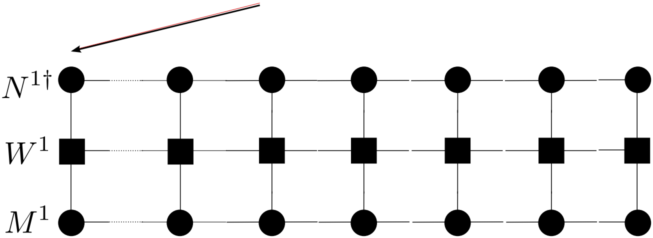

Spin Symmetry Adaptation: MPS and MPO Put Together

$$\boldsymbol{F}_{i'j'}^{[a']}(l+1) = \sum_{aijkss'} \text{Wigner-9j} \begin{bmatrix} jsj' \\ aka' \\ is'i' \end{bmatrix} \boldsymbol{M}_{i'i}^{[s']^\dagger} \boldsymbol{W}_{aa'}^{[k]^{ss'}} \boldsymbol{F}_{ij}^{[a]}(l) \boldsymbol{M}_{j'j}^{[s]}$$

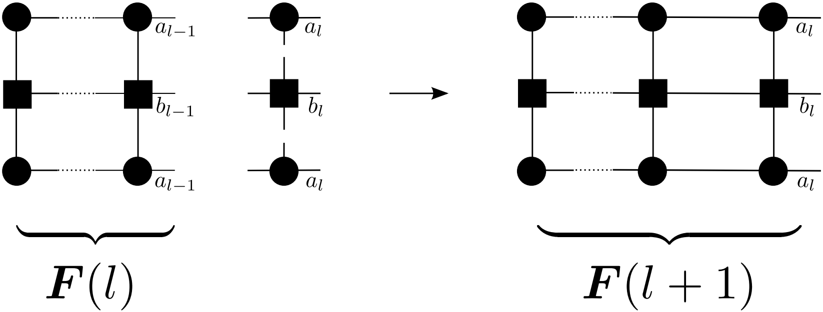

S. Keller, M. Reiher, J. Chem. Phys. 144, 134101 (2016)

Local part of the eigenvalue problem

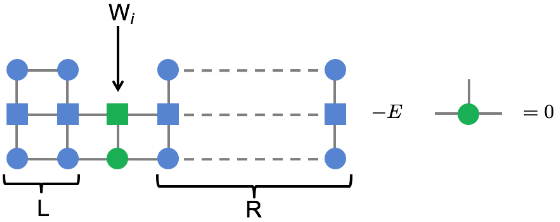

$$\sum_{\sigma_i'}\sum_{a_{i-1}'a_i'}\sum_{b_{i-1}b_i} L_{b_{i-1}}^{a_{i-1},a_{i-1}'} W_{b_{i-1},b_i}^{\sigma_i,\sigma_i'} R_{b_i}^{a_i,a_i'} M_{a_{i-1}',a_i'}^{\sigma_i'} - E M_{a_{i-1},a_i}^{\sigma_i'} = 0$$

- one-site DMRG
- **M**$^{\sigma_i}$ has dimension 4m^2

$\downarrow$ rewrite **M**$^{\sigma_i}$ as vector *v*

$$H\nu - E\nu = 0$$

U. Schollwöck, *Ann. Phys.* (**2011**), *326*, 96.

DMRG – ground state search

Find optimal approximation to $E^{(k)} = \frac{\langle \Psi^{(k)} | \hat{H} | \Psi^{(k)} \rangle}{\langle \Psi^{(k)} | \Psi^{(k)} \rangle}$

by optimizing the entries in $\mathbf{M}^{(k)\sigma_i}$.

Extreme sparsity requires:

- sparse, iterative eigensolvers that aim at the ground state (Jacobi-Davidson)
- in general an iterative procedure with decimation steps

Graphical representation of the standard eigenvalue problem:

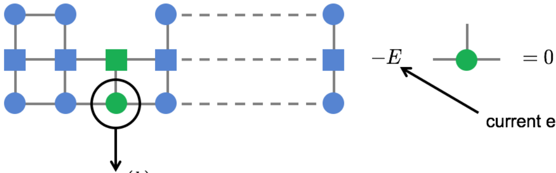

current estimate of ground state energy

entries of $\mathbf{M}^{(k)\sigma_3}$ are optimized

U. Schollwöck, *Ann. Phys.* (**2011**), *326*, 96.

DMRG – ground state search

Sketch of sweep algorithm:

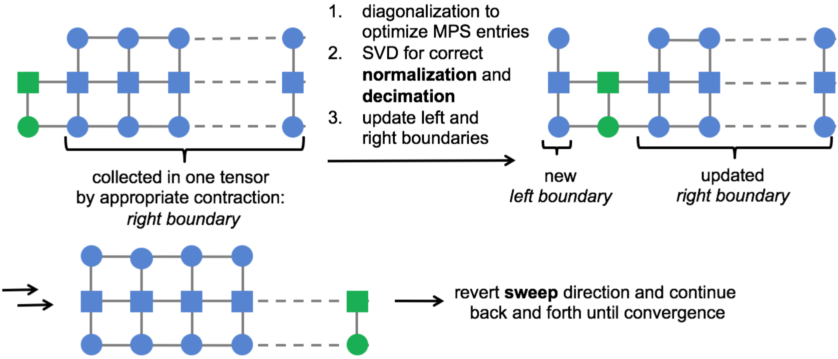

1. diagonalization to optimize MPS entries
2. SVD for correct **normalization** and **decimation**
3. update left and right boundaries

collected in one tensor by appropriate contraction: *right boundary*

new *left boundary*

updated *right boundary*

revert **sweep** direction and continue back and forth until convergence

- decimation step **reduces scaling from exponential to polynomial**
- full-CI solution is approximated in a least-squares sense

U. Schollwöck, *Ann. Phys.* (**2011**), *326*, 96.

DMRG – excited states

sparsity requires eigensolvers that are efficient only for the **ground state**

⟶ is DMRG a ground state method?

ground state search in the space orthogonal to lower lying states

⟶ excited states

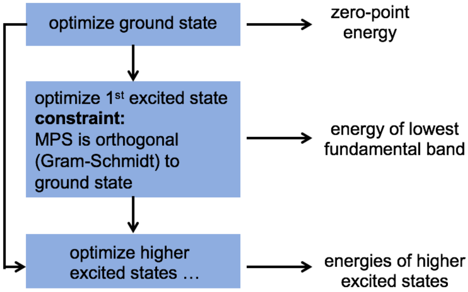

optimize ground state ⟶ zero-point energy

optimize 1st excited state **constraint:** MPS is orthogonal (Gram-Schmidt) to ground state ⟶ energy of lowest fundamental band

optimize higher excited states … ⟶ energies of higher excited states

alternative approach

- root-targeting through diagonalization with lower bound on energy allows direct targeting of excited states
- can be fully parallelized
- successfully implemented and tested and vDMRG

Other Options: Tensor Network States (TNS)

$$\Psi_{el}^{\mathrm{TNS}} = \sum_{i_1 i_2 \ldots i_n} \prod_{i}^{n} \prod_{j \leq i} f_{ij}^{I[i]I[j]} \underbrace{|i_1\rangle \otimes |i_2\rangle \otimes \cdots \otimes |i_n\rangle}_{|I\rangle} \tag{68}$$

- Idea: Rewrite CI coefficient tensor by reducing number of variational parameters (still obtain qualitatively correct wave function).

- **TNS originally proposed for simple** *Spin Hamiltonians*:
  - String-Bond States

N. Schuch, M. Wolf, F. Verstraete, J. I. Cirac, *Phys. Rev. Lett.* **2008** *100* 040501

  - Entangled-Plaquette States

F. Mezzacapo, N. Schuch, M. Boninsegni, J. I. Cirac **2009** arXiv:0905.3898v3

  - Correlator-Product States

H. J. Changlani, J. M. Kinder, C. J. Umrigar, G. K.-L. Chan, **2009** arXiv:0907.4646v1

Complete-Graph Tensor Network States (CG-TNS)

- First implementation of TNS for full quantum-chemical Hamiltonian
- Considering *all* pairs of parameters f_{ij}: CG-TNS
- Parameters optimized with Monte Carlo techniques
- First studied for methylene and ozone; S/T splitting in ozone:

	$\mathrm{E}_{\mathrm{S}=0}/E_h$	$\mathrm{E}_{\mathrm{S}=1}/E_h$	ΔE/kcalmol^{-1}
HF	−224.282 841	−224.357 167	46.6
CASCI	−224.384 301	−224.416 172	20.0
CG-TNS	−224.381 648	−224.412 775	19.5

K. H. Marti, B. Bauer, M. Reiher, M. Troyer, F. Verstraete, New J. Phys. *12* **2010** 103008

Optimization by Variational Quantum Monte Carlo

$$\Psi_{el}^{\mathrm{TNS}} = \sum_{i_1 i_2 \ldots i_N} \prod_i^N \prod_{j \leq i} f_{ij}^{I[i]I[j]} \underbrace{|I\rangle}_{|i_1 i_2 \ldots i_N\rangle} = \sum_I W(I)|I\rangle$$

$$E = \langle E(I)\rangle = \frac{1}{Z}\sum_I W^2(I)E(I) \quad \text{where} \quad Z = \sum_I W^2(I)$$

$$E(I) = \sum_{I'} \frac{W(I')}{W(I)}\langle I'|H|I\rangle$$

- The energy can be evaluated using importance sampling of the configurations $|I\rangle$ according to the weight $W^2(I)$.

A. W. Sandvik, G. Vidal, *Phys. Rev. Lett.* **2007** *99* 220602

CG-TNS for Transition Metal Compounds

- CG-TNS will be efficient if the molecular structure supports the ansatz (clusters!)
- Problem: One must avoid the explicit construction of all CSFs
- First feasibility test: tetraqua-cobalt
  K. H. Marti, M. Reiher, *PCCP 13* (2011) 6750

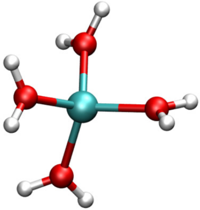

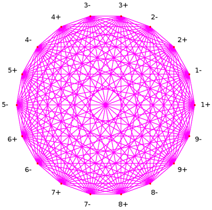

–1676.566 252 E_h

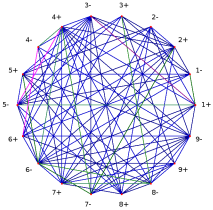

–1685.278 226 E_h

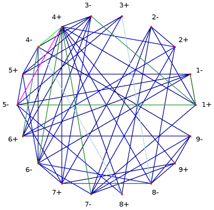

–1685.278 549 E_h

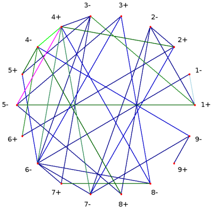

–1685.278 641 E_h

	Hartree–Fock	CAS(9,9)-SCF	CG-TNS
E_{el} / Hartree	−1685.235 055	−1685.293 744	−1685.279 408
Var. Parameters		7056	684

Current Status

- tree tensor network states (TTNS; Legeza, Chan, ...)
- general problem: efficient optimization schemes required
- most promising solution: utilize principles of the DMRG algorithm (most efficiently exploited in an MPS/MPO framework)
- we extended CG-TNS to 3-site correlators (explosion of parameters!)

  A. Kovyrshin, M. Reiher, *NJP 18* (2016) 113001
- ... however, it can only be made accurate and efficient if entanglement-based correlator selection is introduced

  A. Kovyrshin, M. Reiher, in preparation
- unique features of (T)TNS: still to be demonstrated at an example that cannot be solved by standard approaches

Lectures 3 & 4: Applications

1. DMRG for Compact Strongly Correlated Molecules: Transition Metal Complexes
2. Concepts of Quantum Information Theory for Electronic Structures and Chemical Bonding
3. Automated CAS choice enabled by DMRG
4. Challenge: Inclusion of Dynamic Correlation
5. vibrational DMRG (vDMRG)

Density Matrix Renormalization Group: Principles

- New wavefunction parametrization:

$$|\Psi\rangle = \sum_{\boldsymbol{\sigma}} c_{\boldsymbol{\sigma}} |\boldsymbol{\sigma}\rangle \quad \longrightarrow \quad |\Psi\rangle = \sum_{\boldsymbol{\sigma}} M^{\sigma_1} M^{\sigma_2} \cdots M^{\sigma_n} |\boldsymbol{\sigma}\rangle$$

- complete active space (CAS) partitioning and iterative sweeping:

- In essence: dimension reduction by least-squares fitting

Does DMRG Work for Compact Molecules?

- Original 'opinion' in the DMRG community:

  Works only for pseudo-one-dimensional, non-compact systems!

- Test for a mononuclear transition metal system CAS(10,10): CoH

m	$E_{singlet}$/E$_h$	$E_{triplet}$/E$_h$	ΔE/kJmol^{-1}
64	−1381.952 054	−1381.995 106	**113.03**
76	−1381.952 063	−1381.995 109	113.02
91	−1381.952 070	−1381.995 110	113.00
109	−1381.952 073	−1381.995 110	112.99
CAS(10,10)	−1381.952 074	−1381.995 110	**112.99**
CASPT2(10,10)	−1382.189 527	−1382.241 333	130.57
DFT/BP86	−1383.504 019	−1383.585 212	213.1
DFT/B3LYP	−1383.202 267	−1383.279 574	203.0

original work to propose DMRG for compact, strongly correlated molecules:

K. Marti, I. Malkin Ondik, G. Moritz, M. Reiher, *J. Chem. Phys 128* (2008) 014104

'Fully-Relativistic' Four-Component DMRG: TlH

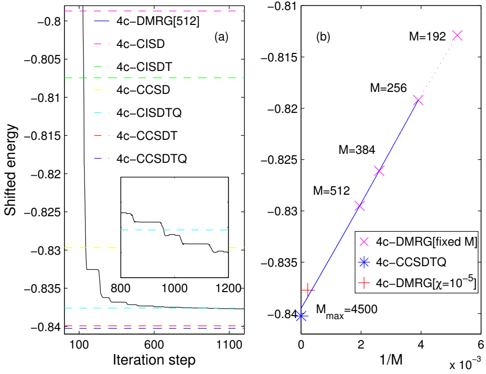

S. Knecht, Ö. Legeza, M. Reiher, *J. Chem. Phys 140* (2014) 041101

method	r_e Å	ω_e $\frac{1}{cm}$	$\omega_e x_e$ $\frac{1}{cm}$
4c-DMRG(14,94)[512]	1.873	1411	26.64
4c-CISD(14,94)	1.856	1462	23.11
4c-CISDTQ(14,94)	1.871	1405	20.11
4c-MP2(14,94)	1.828	1546	47.27
4c-CCSD(14,94)	1.871	1405	19.36
4c-CCSD(T)(14,94)	1.873	1400	23.52
4c-CCSDT(14,94)	1.873	1398	22.28
4c-CCSDT(Q)(14,94)	1.873	1397	21.01
4c-CCSDTQ(14,94)	1.873	1397	22.24
CCSD(T)[a]	1.876	1385	n/a
CCSD(T)[b]	1.877	1376	n/a
MRD-CI[c]	1.870	1420	n/a
SO-MCQDPT[d]	1.876	1391	29.42
experiment[e]	1.872	1390.7	22.7

[a] 4c-DC CCSD(T) [14 electrons], Visscher et al. 2001.

[b] 4c-DC-Gaunt CCSD(T) [36 electrons], Visscher et al. 2001.

[c] GRECP spin-orbit MRD-CI, Titov et al. 2000.

[d] model-core potential spin-orbit MCQDPT, Zeng et al. 2010.

The Cu_2O_2-Torture Track

- Standard CASSCF fails for large CASs relevant in polynuclear clusters
- Example: two different isomers of dinuclear copper clusters

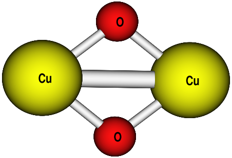

1

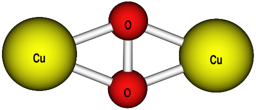

2

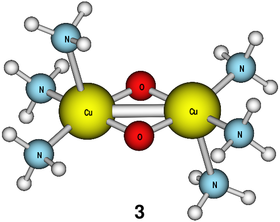

3

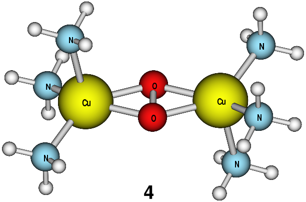

4

C. J. Cramer, M. Włoch, P. Piecuch, C. Puzzarini, L. Gagliardi *J. Phys. Chem. A 110* (2006) 1991

Energies of Isomeric Dinuclear Copper Clusters

- CASSCF fails since large CASs needed for clusters

  K. Marti, I. Malkin Ondik, G. Moritz, M. Reiher, *JCP 128* (2008) 014104

- results with new code and including noise:

  44 active orbitals, 26 electrons, basis set: Cu ECP10MDF, O ANO-Sm, charge: +2

  K. Marti, M. Reiher, *Z. Phys. Chem. 224* (2010) 583

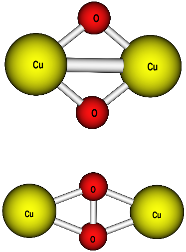

m	E_{bisoxo}/E_h	E_{peroxo}/E_h	$\Delta E/\mathrm{kJmol}^{-1}$
DMRG(m=32)	−541.440 272	−541.478 196	99.6
DMRG(m=44)	−541.446 006	−541.483 405	98.2
DMRG(m=64)	−541.458 021	−541.497 468	103.6
DMRG(m=128)	−541.473 082	−541.514 702	109.3
RASPT2(24,28)[a]			119.66

[a] P. Å. Malmqvist, et al. *J. Chem. Phys 128* (2008) 204109

- What is the fully converged DMRG result for this system?

  → Large-scale DMRG: **149 kJ/mol** Y. Kurashige, T. Yanai, *J. Chem. Phys. 130* (2009) 234114 ... Final answer ?

Torture Track: $[Cu_2O_2]^{2+}$

Ref.,method	E_{bisoxo}	E_{peroxo}	ΔE
'Standard' methods			
A),CASSCF(16,14)	−541.50307	−541.50345	1
A),CASPT2(16,14)	−542.06208	−542.06435	6
A),bs-B3LYP	−544.19419	−544.27844	221
B),RASPT2(24,28)			120
Previously published DMRG energies			
C),DMRG(26,44)[800]	−541.46779	−541.49731	78
D),DMRG(26,44)[128]	−541.47308	−541.51470	109
E),DMRG(32,62)[2400]	−541.96839	−542.02514	149
F),DMRG(28,32)[2048]-SCF	−541.76659	−541.80719	107
F),DMRG(28,32)[2048]-SCF/CT			113
our latest DMRG results with QIT, without noise			
G), DMRG(26,44)[256/1024/10^{-5}]	−541.53853	−541.58114	112

A) C. J. Cramer *et al.*, *J. Phys. Chem. A 110* (2006) 1991; B) P. A. Malmqvist *et al.*, *J. Chem. Phys 128* (2008) 204109; C) K. Marti, *et al.*, *J. Chem. Phys 128* (2008) 014104; D) K. Marti, M. Reiher, *Z. Phys. Chem. 224* (20109 583; E) Y. Kurashige, T. Yanai, *J. Chem. Phys. 130* (2009) 234114; F) T. Yanai *et al.*, *J. Chem. Phys. 132* (2010) 024105; **G) G. Barcza** ***et al.*****,** *Phys. Rev. A 83* **(2011) 012508**

Analyzing DMRG and correlated wave functions with concepts from quantum information theory

Entanglement Measures from Grand Canonical RDMs

- Measure for entanglement of states on orbital i with those defined on (orbital) environment: Ö. Legeza, J. Sólyom, *Phys. Rev. B* **2003**, *68*, 195116.

von-Neumann-type single-orbital entropy

$$s(1)_i = -\sum_{\alpha=1}^{4} \omega_{\alpha,i} \ln \omega_{\alpha,i}$$

($\omega_{\alpha,i}$ eigenvalues of 1o-RDM of spatial orbital i — states defined on all other orbitals are traced out)

- Entanglement of states on orbitals i **and** j with those in environment:

von-Neumann-type two-orbital entropy

$$s(2)_{ij} = -\sum_{\alpha=1}^{16} \omega_{\alpha,ij} \ln \omega_{\alpha,ij}$$

($\omega_{\alpha,ij}$ eigenvalues of 2o-RDM of two spatial orbitals i and j — sub-states defined on all other orbitals traced out)

Entanglement Measures for Embedded Subsystems

- $s(2)_{ij}$ contains also the 'on-site' entropies for the two orbitals

⇒ Subtract these contributions to obtain the 'inter-orbital entropy':

J. Rissler, R.M. Noack, S.R. White, *Chem. Phys.* **2006**, *323*, 519.

Mutual information

$$I_{ij} \propto s(2)_{ij} - s(1)_i - s(1)_j$$

- Advantage over natural occupation numbers:
  - more information,
  - better spread of measures for different electron-correlation classes,
  - system specificity by relating to largest entropy value

Connection between *n*-particle RDM and 1- and 2-orbital RDM

Information exchange (entanglement) between two subsystems *A* and *B* of a bipartite system ⟶ von Neumann entropy

$$S_{A|B} = -\mathrm{tr}_B(\rho \ln \rho) \qquad \rho: \text{ density matrix of the combined system } (A+B)$$

single-orbital entropy: *A* (single orbital), *B* (all other orbitals)

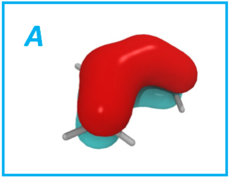

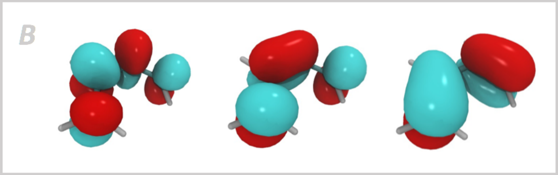

Ö. Legeza, J. Solyom, „Optimizing the density-matrix renormalization group using quantum information entropy", *Phys. Rev. B* **2003**, *68*, 195116.
Ö. Legeza, J. Solyom, „ Quantum data compression, quantum information generation, and the density-matrix renormalization-group method ", *Phys. Rev. B* **2004**, *70*, 205118.
J. Rissler, R. M. Noack, S. R. White, „Measuring orbital interaction using quantum information theory", *Chem. Phys.* **2006**, *323*, 519.

Connection between *n*-particle RDM and 1- and 2-orbital RDM

single-orbital entropy: *A* (single orbital), *B* (all other orbitals)

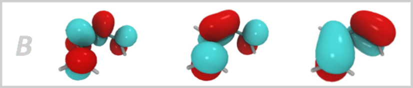

local states on single orbital (*A*):

$$\{|\alpha\rangle\} = \{|\rangle, |\uparrow\rangle, |\downarrow\rangle, |\uparrow\downarrow\rangle\}$$

states on all other orbitals (*B*):

$$\{|\mathbf{n}\rangle\}$$

one-orbital reduced density matrix (1o-RDM):

$$\rho^{(1)}_{\alpha,\alpha'}(A) = \sum_{\mathbf{n}} \langle\mathbf{n}|\langle\alpha|\Psi\rangle\langle\Psi|\alpha'\rangle|\mathbf{n}\rangle \longrightarrow s_A(1) = -\sum_{\alpha=1}^{4} \rho^{(1)}_{\alpha,\alpha}(A)\ln\rho^{(1)}_{\alpha,\alpha}(A)$$

$$s_A(1) \equiv -\sum_{\alpha=1}^{4} \omega_{\alpha,A}\ln\omega_{\alpha,A}$$

J. Rissler, R. M. Noack, S. R. White, *Chem. Phys.* **2006**, *323*, 519.

Connection between *n*-particle RDM and 1- and 2-orbital RDM

elements of the spin-dependent 1-RDM: $\gamma_{AA'} = \langle\Psi|a^\dagger_A a_{A'}|\Psi\rangle$

elements of the spin-dependent 2-RDM: $\Gamma_{AA'A''A'''} = \langle\Psi|a^\dagger_A a^\dagger_{A'} a_{A''} a_{A'''}|\Psi\rangle$

$$\rho_A^{(1)} = \begin{array}{c} \begin{array}{cccc} - & \uparrow & \downarrow & \uparrow\downarrow \end{array} \\ \left(\begin{array}{cccc} 1-\gamma_{AA}-\gamma_{\bar{A}\bar{A}}+\Gamma_{A\bar{A}A\bar{A}} & 0 & 0 & 0 \\ 0 & \gamma_{AA}-\Gamma_{A\bar{A}A\bar{A}} & 0 & 0 \\ 0 & 0 & \gamma_{\bar{A}\bar{A}}-\Gamma_{A\bar{A}A\bar{A}} & 0 \\ 0 & 0 & 0 & \Gamma_{A\bar{A}A\bar{A}} \end{array}\right) \end{array} \begin{array}{c} - \\ \uparrow \\ \downarrow \\ \uparrow\downarrow \end{array}$$

A indicates α spin, $\bar{A}$ indicates β spin

- diagonal because of particle and spin symmetries
- similar expressions connect the 2o-RDM with elements of the 1,2,3- and 4-RDM

K. Boguswaski, P. Tecmer, *Int. J. Quantum Chem.* **2015**, *115*, 1289.

What does the single-orbital entropy measure?

The single-orbital entropy measures the *deviation* from a pure state defined on a subsystem (orbital) due to the interaction with states defined on the environment (all other orbitals)!

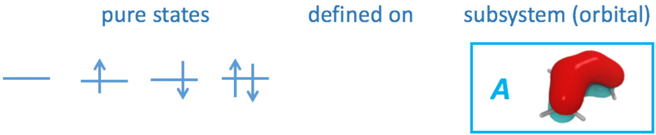

For a single determinant, the orbital state is pure → no single-orbital entropy

In configuration interaction, several configurations contribute to the total wave function and lead to a *deviation* from a pure single-orbital state.

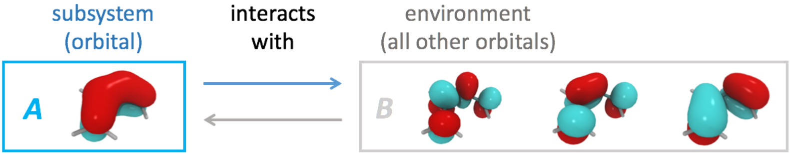

This is in complete analogy to the thermodynamical definition of entropy.

Entanglement Measures

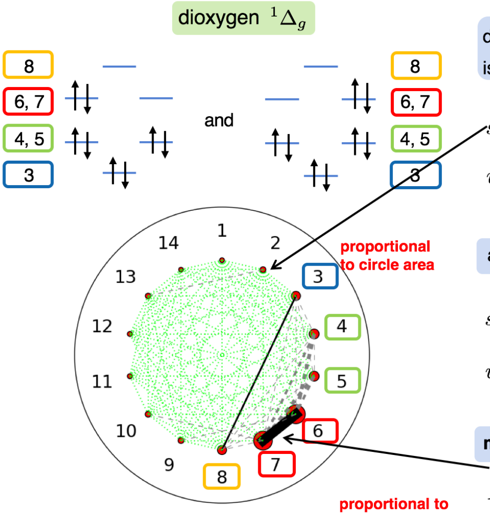

proportional to thickness of connecting lines

C.J. Stein, M. Reiher, *Chimia* **2017**, *4*, 170.
arXiv: 1702.00450

deviation from a pure state α (—, ↑, ↓, ↑↓) is measured by **single-orbital entropy**

$$s_i(1) = -\sum_{\alpha=1}^{4} w_{\alpha,i} \ln w_{\alpha,i}$$

$w_{\alpha,i}$: eigenvalue of the reduced one-orbital density matrix for orbital *i*

analogously for two orbitals: **two-orbital entropy**

$$s_{ij}(2) = -\sum_{\alpha=1}^{16} w_{\alpha,ij} \ln w_{\alpha,ij}$$

$w_{\alpha,ij}$: eigenvalue of the reduced two-orbital density matrix for orbitals *i, j*

mutual information

$$I_{ij} = \frac{1}{2}\left[s_i(1) + s_j(1) - s_{ij}(2)\right](1 - \delta_{ij})$$

Orbital entanglement and locality of electron correlation

- localized π/ π* interaction is an example of local electron correlation
- conjugated π/ π* orbitals should delocalize the correlation to some extent

⟶ Can this be analyzed with orbital entanglement measures?

buta-1,3-diene

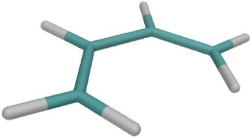

- planar
- conjugated π-system
  (4 electrons in 4 orbitals)

penta-1,4-diene

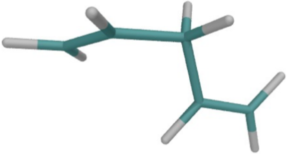

- additional CH_2 unit prevents planarity
- 2 separate π-systems
  (4 electrons in 4 orbitals)

C. J. Stein, M. Reiher, *to be published*.

Generation of different types of orbitals

1. CAS(4,4)SCF calculation in Molcas 8

   → delocalized orbitals with a π/π* active space

2. Pipek-Mezey localization in 4 orbital active space

   → completely localized orbitals (2p_z-like atomic orbitals)

3. a) Pipek-Mezey localization for 2 occupied active orbitals

   and

   b) Cholesky localization followed by another Pipek-Mezey localization for the 2 unoccupied active orbitals

   → split-localized orbitals (π/ π* pairs)

C. J. Stein, M. Reiher, *to be published.*

Three types of orbitals for buta-1,3-diene

delocalized

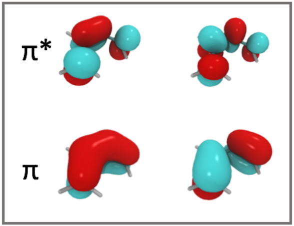

converged DMRG-CI energy:
-155.0812146 Hartree

split-localized

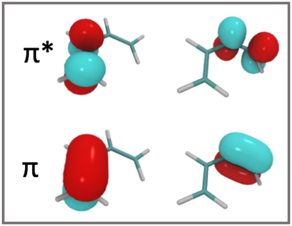

converged DMRG-CI energy:
-155.0812146 Hartree

completely localized

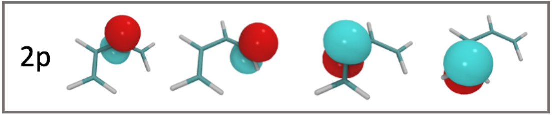

converged DMRG-CI energy:
-155.0812146 Hartree

C. J. Stein, M. Reiher, *to be published*.

Three types of orbitals for penta-1,4-diene

delocalized

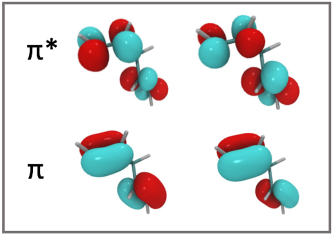

converged DMRG-CI energy:
-194.1332521 Hartree

split-localized

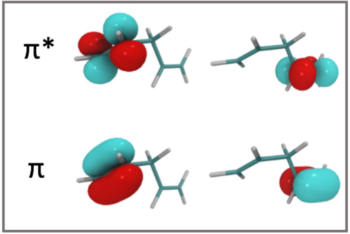

converged DMRG-CI energy:
-194.1332521 Hartree

completely localized

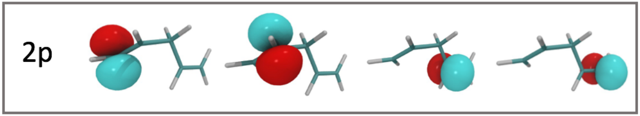

converged DMRG-CI energy:
-194.1332521 Hartree

C. J. Stein, M. Reiher, *to be published*.

Entanglement for delocalized orbitals

from a converged DMRG-CI calculation with 4 electrons in 4 orbitals

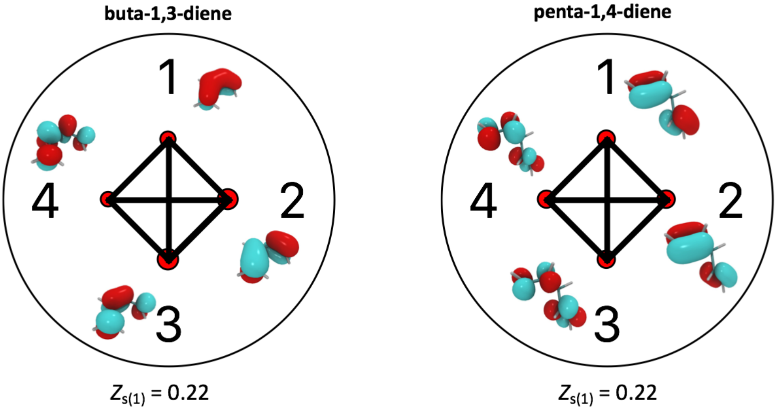

$Z_{s(1)} = 0.22$ $Z_{s(1)} = 0.22$

- almost indistinguishable entanglement pattern for both molecules
- all orbitals equally entangled

C. J. Stein, M. Reiher, *to be published.*

Entanglement for split-localized orbitals

from a converged DMRG-CI calculation with 4 electrons in 4 orbitals

buta-1,3-diene

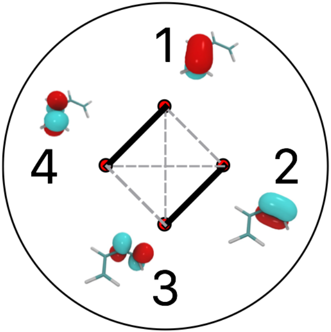

$Z_{s(1)} = 0.16$

penta-1,4-diene

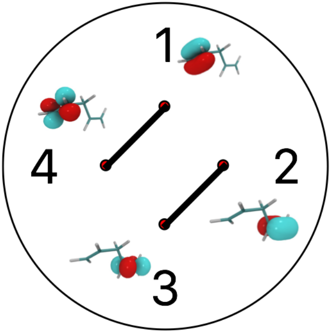

$Z_{s(1)} = 0.13$

- strongest mutual information for paired π/π * orbitals
- conjugation is reflected in entanglement between neighboring pairs (buta-1,3-diene)

C. J. Stein, M. Reiher, *to be published.*

Entanglement for completely localized orbitals

from a converged DMRG-CI calculation with 4 electrons in 4 orbitals

buta-1,3-diene

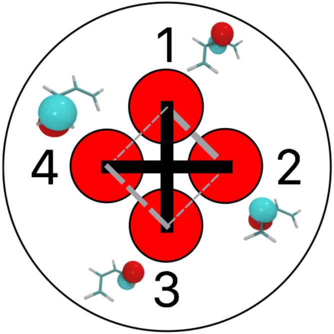

$Z_{s(1)} = 0.94$

penta-1,4-diene

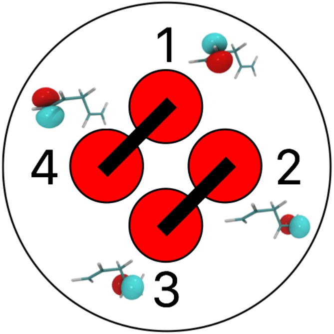

$Z_{s(1)} = 0.94$

- huge single-orbital entropies
- strongest mutual information between AOs forming the π and π * orbitals
- penta-1,4-diene: no “inter-pair” mutual information ⟶ no conjugation

C. J. Stein, M. Reiher, *to be published*.

Entanglement Measures can Monitor Bond Breaking/Formation Processes: Dinitrogen

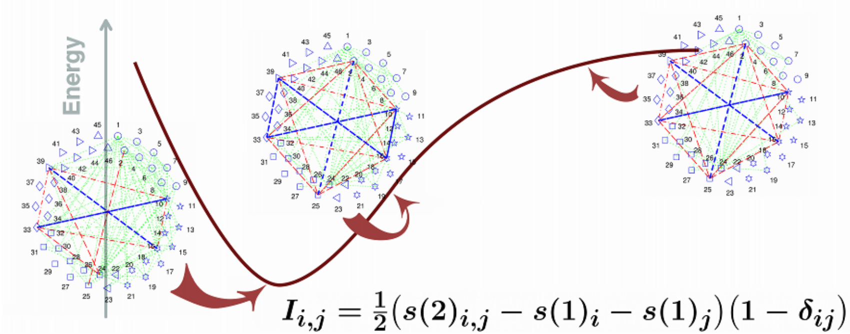

$$I_{i,j} = \frac{1}{2}\big(s(2)_{i,j} - s(1)_i - s(1)_j\big)\big(1 - \delta_{ij}\big)$$

K. Boguslawski, P. Tecmer, G. Barcza, O. Legeza, M. Reiher, *J. Chem. Theory Comput.* *9* **2013** 2959–2973 [arxiv: 1303.7207]

Bond Breaking in Dinitrogen at 1.12 Ångström

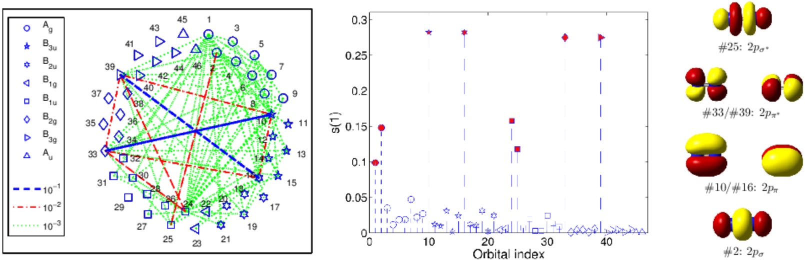

Mutual information

Single orbital entropy

(a) $d_{\mathrm{NN}} = 1.12\text{Å}$

Part of entanglement is already encoded in molecular orbitals changing with the structure !

Atomic-like non-orthogonal basis fcts. exhibit large entanglement measures among each other.

Bond Breaking in Dinitrogen at 1.69 Ångström

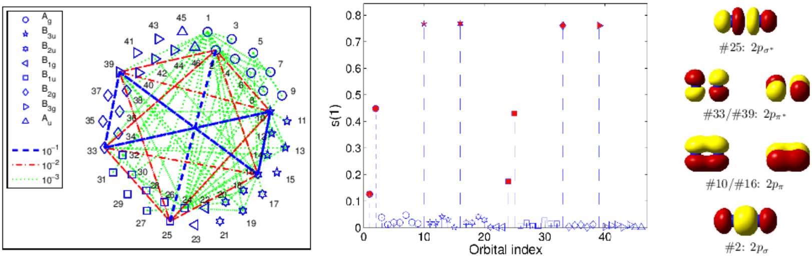

Mutual information

Single orbital entropy

(b) $d_{\mathrm{NN}} = 1.69$Å

Part of entanglement is already encoded in molecular orbitals changing with the structure !

Atomic-like non-orthogonal basis fcts. exhibit large entanglement measures among each other.

Bond Breaking in Dinitrogen at 2.22 Ångström

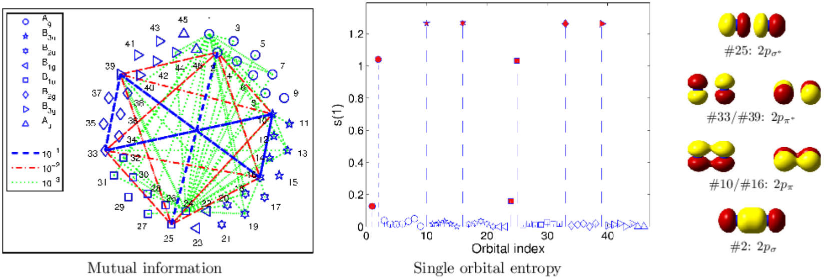

Mutual information

Single orbital entropy

(d) $d_{\mathrm{NN}} = 2.22$Å

Part of entanglement is already encoded in molecular orbitals changing with the structure !

Atomic-like non-orthogonal basis fcts. exhibit large entanglement measures among each other.

Bond Breaking in Dinitrogen at 3.18 Ångström

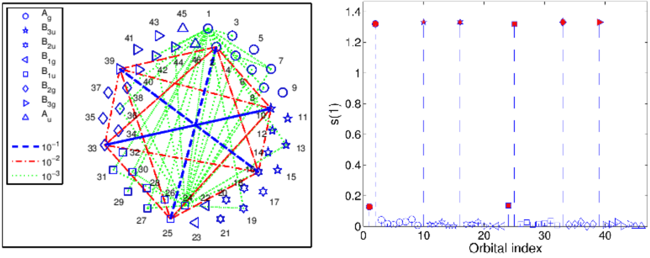

Mutual information

Single orbital entropy

(f) $d_{\mathrm{NN}} = 3.175\text{Å}$

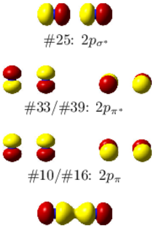

Part of entanglement is already encoded in molecular orbitals changing with the structure !

Atomic-like non-orthogonal basis fcts. exhibit large entanglement measures among each other.

Entanglement relates to Electron Correlation

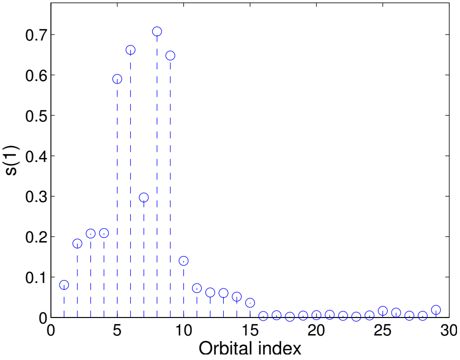

K. Boguslawski, P. Tecmer, Ö. Legeza, M. Reiher,

J. Phys. Chem. Lett. **2012**, *3*, 3129.

- Three groups of orbitals
  - $\Rightarrow$ large single orbital entropy
  - $\Rightarrow$ medium single orbital entropy
  - $\Rightarrow$ tiny single orbital entropy
- Configurations belonging to the third block have small C_I $\Rightarrow$ important for dynamic correlation
- Note: more structure than in spectrum of 1e-RDM

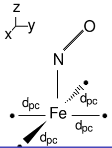

- 4 point charges in xy-plane at d$_{\rm pc}$ $= 1.133$ Å
- Natural orbital basis: CAS(11,14)SCF/cc-pVTZ
- DMRG(13,29) with DBSS ($m_{\rm min} = 128, m_{\rm max} = 1024$)

How to cope with the active space selection problem ?

How to choose an active space? — Insights

- "… the choice of the active space actually used in more complex systems is **highly subjective and can lead to serious problems**."

  R. D. Bach in *The Chemistry of Peroxides*, Z. Rappoport (Ed.), John Wiley & Sons, (2006) 4.

- "CAS-based methods are another alternative, although the selection of the active space is a **tremendous challenge.**"

  Y. Shao, L. Molnar, Y. Jung, J. Kussmann, C. Ochsenfeld *et al.*, *Phys. Chem. Chem. Phys.*, 8, (2006) 3172–3191.

- "Choosing the "correct" active space for a specific application is by no means trivial; **often the practitioner must "experiment"** with different choices in order to assess adequacy and convergence behavior. While every chemical system poses its own challenges, **certain rules of thumb apply.**"

  P. Å. Malmqvist, K. Pierloot, A. R. M. Shahi, C. J. Cramer, L. Gagliardi, *J. Chem. Phys.*, 128, (2008) 204109.

How to choose an active space? — Recipes

- B. O. Roos (1989)

  The Complete Active Space Self-Consistent Field Method and Its Applications in Electronic Structure Calculations; in *Ab Initio Methods in Quantum Chemistry*, K.P. Lawley (Ed.), John Wiley & Sons Ltd., 399–446.

  \- most active orbitals should appear paired (one highly occupied and one corresponding almost empty orbital)

  \- conjugated and aromatic bonds should be included in the CAS

  \- both the bonding and antibonding orbitals of a bond that is broken have to be included

  \- orbitals describing C-H bonds are not to be included in active space

- ... more rules in later papers by the Lund group

How to choose an active space? — Recipes

- M. W. Schmidt, M. S. Gordon (1998)

  The Construction and Interpretation of MCSCF Wavefunctions; *Annu. Rev. Phys. Chem.* 49, 233–266.

  - choice of active space is based on generalized valence bond diagrams

- K. Pierloot (2003)

  The CASPT2 Method in Inorganic Electronic Spectroscopy: from Ionic Transition Metal Complexes to Covalent Actinide Complexes; *Mol. Phys.* 101, 2083–2094.

  - description of double-shell effect and its importance for CASPT2

How to choose an active space? — Recipes

- A. Kerridge (2015)
  The Complete-Active-Space Self-Consistent-Field Approach and Its Application to Molecular Complexes of the f-Elements; in *Computational Methods in Lanthanide and Actinide Chemistry* M. Dolg (Ed.), John Wiley & Sons Ltd., 138–139.

  - $4f$-, $5d$- and $6s$-orbitals of lanthanides should be included
  - $5f$-, $6d$- and $7s$-orbitals of actinides should be included
  - for highly charged complexes, $5f$-orbitals only

- F. Krausbeck, D. Mendive-Tapia, A. Thom, M. Bearpark (2014)
  Choosing RASSCF Orbital Active Spaces for Multiple Electronic States; *Comput. Theor. Chem.* 1040-1041, 14–19.

  - active space for CASSCF and RASSCF calculations is chosen according to natural occupation numbers derived from averaged SCF density matrix obtained from calculations for different electronic states

How to choose an active space? — Recipes

- J. M. Bofill, P. Pulay (1989)
  J. Chem. Phys. 90, 3637–3646.

  - unrestricted Hartree-Fock natural orbitals (UNOs) are used as starting orbitals for CASSCF calculations
  - orbitals with occupation numbers between 0.02 and 1.98 are selected for the active space

  - the idea has been explored further by comparison to DMRG results:

  S. Keller, K. Boguslawski, T. Janowski, M. Reiher, P. Pulay (2015)
  J. Chem. Phys. 142, 244104.

Can one choose the CAS in an automated way?

Exploit Two Advantages of DMRG for the CAS choice

- DMRG is iterative
- DMRG can handle large CAS sizes

$\Longrightarrow$ ... toward an automated CAS determination

requires selection criterion: entanglement entropy measures!

Automated CAS selection? Black-box CASSCF?

... reduce the human time by automatizing manual selection (if manual selection fails, the automated protocol will have a problem, too)

Partially converged entanglement information is sufficient

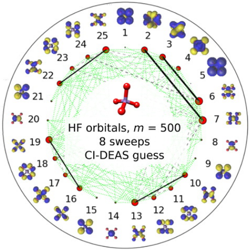

E = -1449.290301 E_H

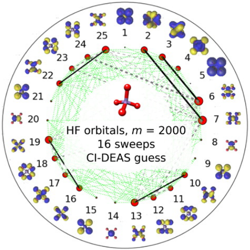

E = -1449.302426 E_H

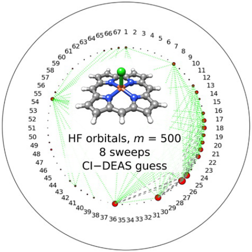

E = -2665.877397 E_H

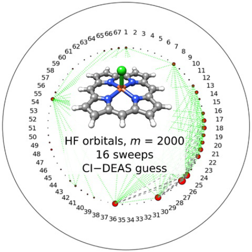

E = -2665.878045 E_H

Automated Orbital Selection Algorithm

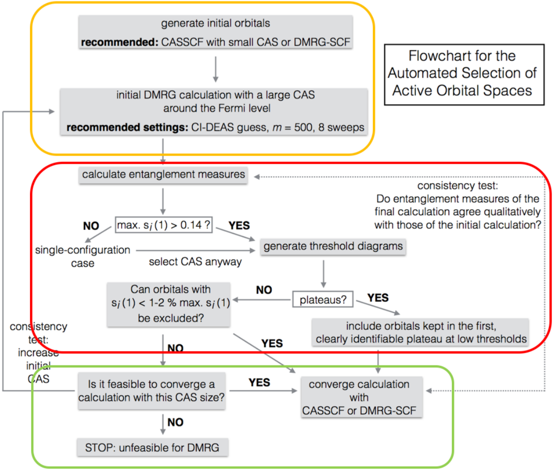

Flowchart for the Automated Selection of Active Orbital Spaces

generate initial orbitals
recommended: CASSCF with small CAS or DMRG-SCF

initial DMRG calculation with a large CAS around the Fermi level
recommended settings: CI-DEAS guess, $m = 500$, 8 sweeps

calculate entanglement measures

max. $s_i(1) > 0.14$?

NO

single-configuration case

select CAS anyway

YES

generate threshold diagrams

plateaus?

NO

Can orbitals with $s_i(1) <$ 1-2 % max. $s_i(1)$ be excluded?

YES

include orbitals kept in the first, clearly identifiable plateau at low thresholds

consistency test: Do entanglement measures of the final calculation agree qualitatively with those of the initial calculation?

YES

NO

consistency test: increase initial CAS

Is it feasible to converge a calculation with this CAS size?

YES

converge calculation with CASSCF or DMRG-SCF

NO

STOP: unfeasible for DMRG

recipe

1. **partially converged DMRG calculation** with a large number of active orbitals
2. **identify “important” orbitals**
3. **converge the calculation** with only “important” orbitals

Stein, C. J., Reiher, M. *JCTC*, **2016**, *12*, 1760.

Entanglement based multi-configurational diagnostic $Z_{s(1)}$

Need for a consistent, formalism-inherent threshold descriptor

Design criteria

- well-defined limits
  (0 = no static correlation,
  1 = max. static correlation);
  note: maximum entropy

$$\sum_{i=1}^{L}[s_i^{\max}(1)] = \sum_{i=1}^{L}\left[-\sum_{\alpha=1}^{4}\left(\frac{1}{4}\ln\frac{1}{4}\right)\right] = L\ln 4$$

- obtained from a qualitatively correct wave function
  (⟷ MC measures from SC wave functions, e.g. T_1 diagnostic)
- intensive, not extensive

Definition and constraints

$$Z_{s(1)} = \frac{1}{L' \ln 4}\sum_{i}^{L'} s_i(1)$$

- $L' \leq L$, where L is restricted to most entangled orbitals selected according to our automated active orbital selection scheme[1];
  otherwise: $\lim_{L' \to \infty} Z_{s(1)} = 0$
- maximum entropy can only be achieved if all possible occupations can be realised with equal weight, which requires one electron per spatial orbital CAS(N,L'=N)

C. J. Stein, M. Reiher, *Mol. Phys.* **2017**, doi: 10.1080/00268976.2017.1288934; arXiv:1609.02617v2 (**2016**)

[1] C. J. Stein, M. Reiher, *JCTC* **2016,** *12*, 1760.

Behavior of $Z_{s(1)}$ upon bond stretching

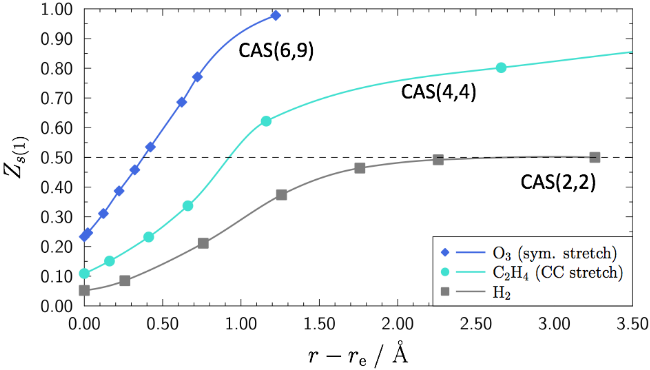

- multi-configurational character increases with bond stretching

- symmetry in H_2 reduces maximum to $Z_{s(1)}^{max} = 0.5$
  ($\rho_{\alpha,\alpha'}(A)$ is 2-dimensional for *gerade* ground-state symmetry;
  → max. entropy: $L \ln 2 = 2 \ln 2$, but $Z_{s(1)}$ defined for general case)

C. J. Stein, M. Reiher, *Mol. Phys.* **2017**, doi: 10.1080/00268976.2017.1288934
arXiv:1609.02617v2 (**2016**)

Size independence of $Z_{s(1)}$

- $Z_{s(1)}$ determines multi-configurational character without artefacts from system size

	methane	propane	pentane	heptane	nonane
$(N,L'=N)$	(8,8)	(20,20)	(32,32)	(44,44)	(56,56)
$Z_{s(1)}$	0.04	0.03	0.03	0.03	0.03

- polyacenes: *multi-configurational character* constant,
  previous results (Chan, Mazziotti, Carter, Yanai, Lischka, Head-Gordon,...):
  diradical character increases with increasing system size

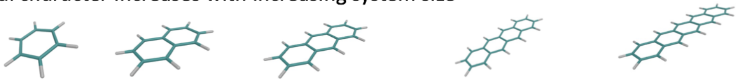

	benzene	naphtalene	anthracene	tetracene	pentacene
$(N,L'=N)$	(6,6)	(10,10)	(14,14)	(18,18)	(22,22)
$Z_{s(1)}$	0.21	0.23	0.24	0.25	0.24

C. J. Stein, M. Reiher, *Mol. Phys.* **2017**, doi: 10.1080/00268976.2017.1288934; arXiv:1609.02617v2 (**2016**)

Basis set dependence of $Z_{s(1)}$

- choice of molecular orbital basis defines static correlation patterns
- example: H_2 in minimal basis with canonical HF orbitals and localized orbitals (Pipek-Mezey localization yields VB basis in a minimal AO basis (STO-3G))

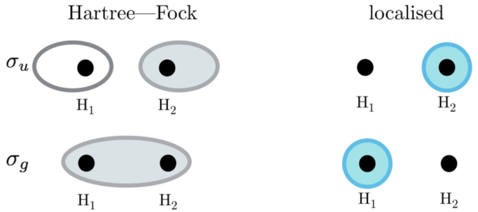

same molecule,

same structure,

only different MO basis!

$$\Psi_{\text{GS}}^{\text{approx.}} = |\sigma_g(\uparrow\downarrow)\rangle$$

single determinant is a good approximation

$$\begin{aligned}\Psi_{\text{GS}}^{\text{approx.}} = 4^{-1/2}[&|1s_{\text{H1}}(\uparrow\downarrow)\rangle + |1s_{\text{H2}}(\uparrow\downarrow)\rangle \\ &+ |1s_{\text{H1}}(\uparrow)1s_{\text{H2}}(\downarrow)\rangle \\ &+ |1s_{\text{H1}}(\downarrow)1s_{\text{H2}}(\uparrow)\rangle]\end{aligned}$$

single determinant is insufficient: multi-configurational problem!

C. J. Stein, M. Reiher, *Mol. Phys.* **2017**, doi: 10.1080/00268976.2017.1288934; arXiv:1609.02617v2 (**2016**)

Basis set dependence of $Z_{s(1)}$

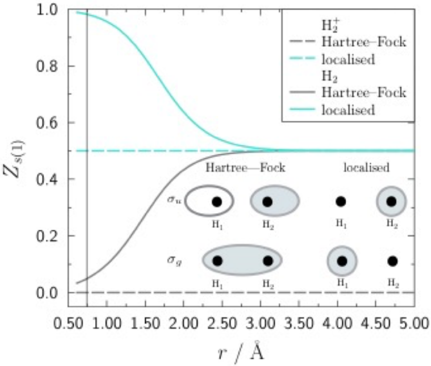

- choice of basis can create multi-configurational character
- H_2^+: only one electron ⟶ constant entropy
- H_2: localized basis ⟶ no symmetry constraint ⟶ max. entropy $L \ln 4$

C. J. Stein, M. Reiher, *Mol. Phys.* **2017**, doi: 10.1080/00268976.2017.1288934; arXiv:1609.02617v2 (**2016**)

Additional remarks on $Z_{s(1)}$

- $Z_{s(1)}$ parallels other multi-configurational diagnostics
  (T1-diagnostic[1], D1-diagnostic[2], HF exchange based diagnostics[3], NOON based diagnostics [4] …)

- typical classification:

  $0 < Z_{\mathrm{s}(1)} < 0.1$ single-configuration

  $0.1 \leq Z_{\mathrm{s}(1)} < 0.2$ intermediate range
  (multi-configurational methods are a safe choice)

  $0.2 \leq Z_{\mathrm{s}(1)} < 1$ pronounced multi-configurational character

- is evaluated without additional cost in our automated active orbital space selection protocol[5]

- guide for the selection of the electronic structure method

C. J. Stein, M. Reiher, *Mol. Phys.* **2017**, doi: 10.1080/00268976.2017.1288934; arXiv:1609.02617v2 (**2016**)
[1] T. J. Lee, P. R. Taylor, *Int. J. Quantum Chem.* **1989**, *36*, 199.
[2] C. L. Janssen, I. M. B. Nielsen, *CPL* **1998**, *290*, 423.
[3] U. R. Fogueri, S. Kozuch, A. Karton, J. M. L. Martin, *Theor. Chem. Acc.* **2012**, *132*, 1291.
[4] O. Tishchenko, J. Zheng, D. G. Truhlar, *JCTC* **2008**, *4*, 1208.
[5] C. J. Stein, M. Reiher, *JCTC* **2016,** *12*, 1760.

Graphical User Interface

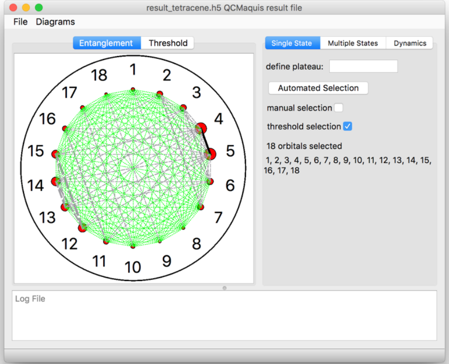

define plateau:

manual selection ☐

threshold selection ☑

18 orbitals selected

1, 2, 3, 4, 5, 6, 7, 8, 9, 10, 11, 12, 13, 14, 15, 16, 17, 18

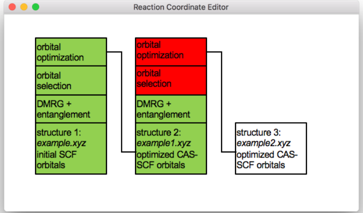

orbital optimization
orbital selection
DMRG + entanglement
structure 1: *example.xyz* initial SCF orbitals

orbital optimization
orbital selection
DMRG + entanglement
structure 2: *example1.xyz* optimized CAS-SCF orbitals

structure 3: *example2.xyz* optimized CAS-SCF orbitals

Black Box DMRG Calculations

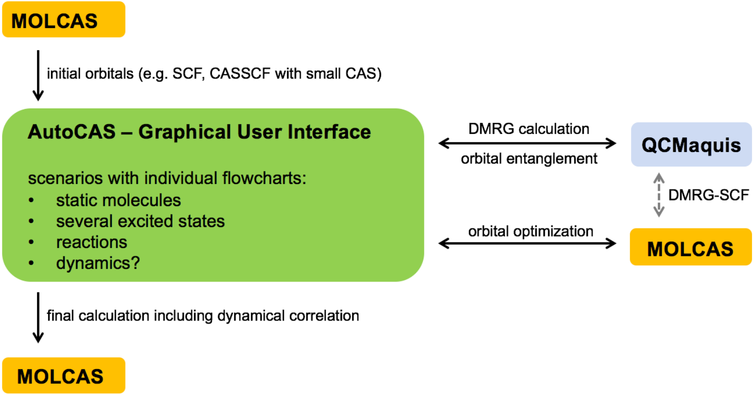

MOLCAS

initial orbitals (e.g. SCF, CASSCF with small CAS)

AutoCAS – Graphical User Interface

scenarios with individual flowcharts:
- static molecules
- several excited states
- reactions
- dynamics?

DMRG calculation

orbital entanglement

QCMaquis

DMRG-SCF

orbital optimization

MOLCAS

final calculation including dynamical correlation

MOLCAS

Same CAS selection for different types of orbitals

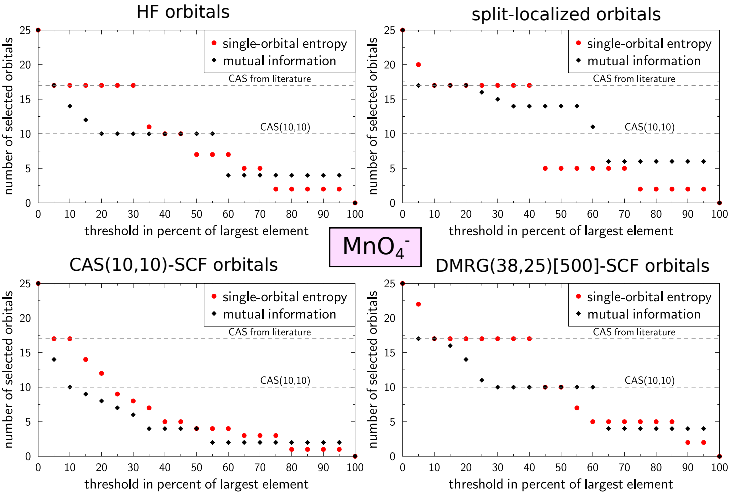

- the same CAS is automatically selected for all orbital bases

Subtle correlation effects are automatically captured

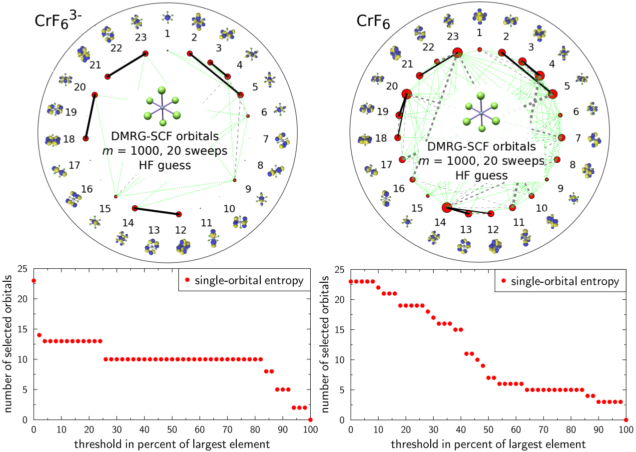

- correlation effects attributed to the covalency of the bonds are automatically accounted for

The $Cu_2O_2^{2+}$ Torture Track

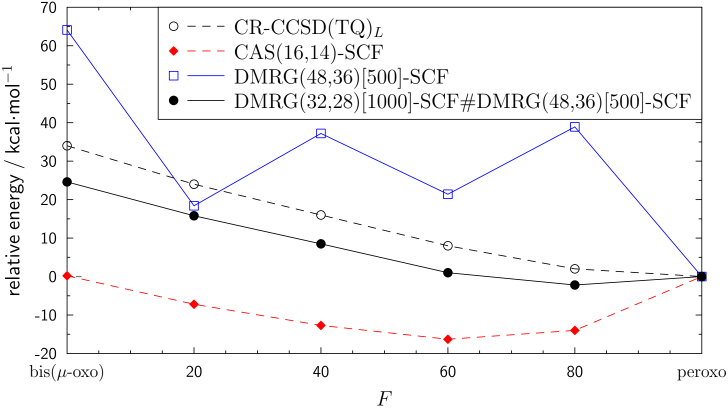

- Coupled cluster and CASSCF data from C. J. Cramer *et al.*, *JPC A* (**2006**), 110, 1991.
- discrepancy to coupled-cluster result can be explained by (still) missing dynamical correlation C. J. Stein, M. Reiher, J. Chem. Theory Comput, **2016**, 12, 1760–1771.

Automated Orbital Selection Along Reaction Coordinates

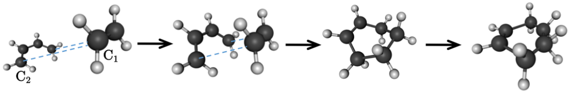

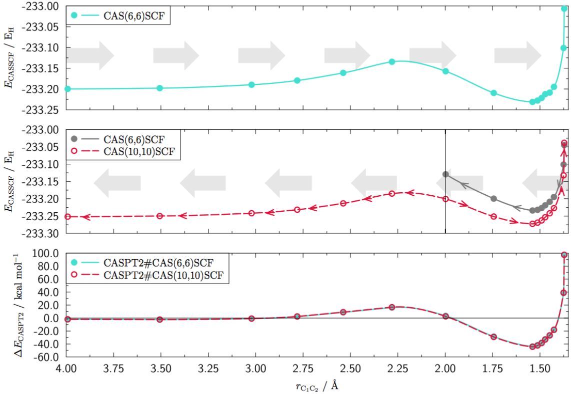

Diels-Alder reaction

- C_s symmetric reaction coordinate (DFT structures)
- direction in which active space is selected plays a role
- this effect is completely leveled out by inclusion of dynamical correlation
- additional orbitals in middle panel indicate a second process

C. J. Stein, M. Reiher, *Chimia* **2017**, *4*, 170.; arXiv: 1702.00450

Need dynamic correlation for quantitative reference data!

Metallocene Double Dissociation Energies

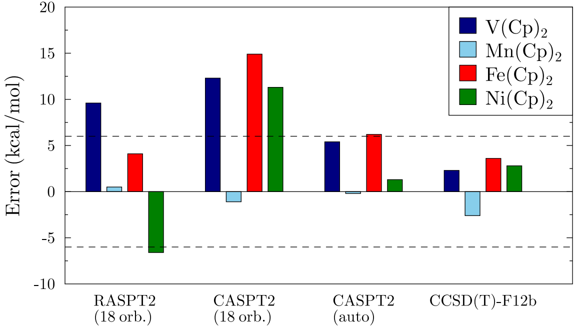

- Double dissociation energies are around 600 kcal/mol!

C. J. Stein, V. von Burg, M. Reiher, J. Chem. Theory Comput, under review [arXiv: 1605.07020]

An Issue of CASPT2: The IPEA Shift

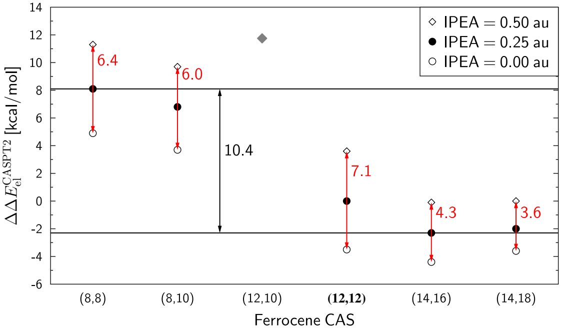

The range of results produced by a modified IPEA shift is comparable to that of a variable CAS size (indicated by horizontal lines)

C. J. Stein, V. von Burg, M. Reiher, J. Chem. Theory Comput, under review [arXiv: 1605.07020]

DMRG–NEVPT2: Singlet–Triplet Gap of Methylene

$E(\tilde{a}^1 A_1)$–$E(\tilde{X}^3 B_1)$ in kcal/mol

	CAS(6,6)	CAS(6,12)	CAS(6,20)
CASSCF	10.53	5.71	9.93
CASSCF/CASPT2	11.87	10.56	10.26
DMRG-SCF	10.53	5.71	9.93
DMRG-SCF/NEVPT2	11.71	9.13	10.17

S. Knecht, E. D. Hedegård, S. Keller, A. Kovyrshin, Y. Ma, A. Muolo, C. J. Stein, M. Reiher, *Chimia* **2016**, 70, 244 [arXiv: 1512.09267]

DMRG–NEVPT2: No approximations for 3- and 4-body RDMs

DFT	PBE: 16.03	PBE0: 17.72

FCI: C. D. Sherrill et al., *J. Chem. Phys.* **1998**,

How to Improve on Dramatic Requirements of Resources?

- cumulant approximation for 3- and 4-particle reduced density matrix in NEVPT2 or CASPT2 D. Zgid, D. Ghosh, E. Neuscamman, G. K.-L. Chan, *J. Chem. Phys.*, **2009**, 130, 194107. & Y. Kurashige, J. Chalupský, T. N. Lan, T. Yanai, *J. Chem. Phys.*, **2014**, 141, 174111.

  - with correct diagonal elements

  - only 4-RDM is approximated

- projection of strongly contracted perturber functions onto a renormalized Hilbert space M. Roemelt, S. Guo, G. K.-L. Chan, *J. Chem. Phys.*, **2016**, 144, 204113.

- alternative approach: minimizing the Hylleraas functional in the space of matrix product states S. Sharma, G. K.-L. Chan, *J. Chem. Phys.*, **2014**, 141, 111101.

- Improve efficiency for integral and RDM evaluation

  L. Freitag, S. Knecht, C. Angeli, M. Reiher, J. Chem. Theory Comput. **2016**, under review [arXiv: 1608.02006]; C. J. Stein, S. Knecht, M. Reiher, in preparation

NEVPT2 for large systems

- Exact four-particle RDM: no cumulant approximations
  - very expensive but doable for active spaces of ≈ 22 orbitals
- Large molecules: Cholesky decomposition for two-electron integrals
  - allows for systems with > 1000 basis functions

$\hookrightarrow$ CD-DMRG-NEVPT2

L. Freitag, S. Knecht, C. Angeli, M. Reiher, JCTC (2016) under review (arXiv:1608.02006)

Spin states of a cobalt tropocoronand complex

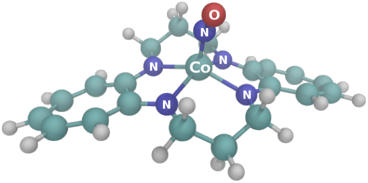

[Co(TC-3,3)(NO)]

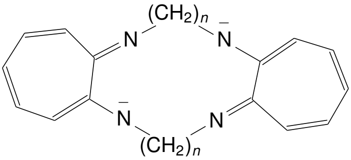

TC-n,n

[Co(TC-n,n)(NO)]

- $n = 4$-6 – diamagnetic
- $n = 3$ – paramagnetic or diamagnetic?

Before Ref. 5: paramagnetic

Ref. 5: diamagnetic (from DFT and new experimental results)

calls for an additional investigation!

L. Freitag, S. Knecht, C. Angeli, M. Reiher, JCTC (2016) under review (arXiv:1608.02006)

[5] Hopmann et al., Inorg. Chem. 2015, 54, 7362

[Co(TC-3,3)(NO)] – spin state energetics

CD-DMRG-NEVPT2[512] (22,22)/ANO-RCC-VTZP (1147 basis functions)

S_0-T_1 gap of [Co(TC-3,3)(NO)] in eV:

SC-NEVPT2	DMRG-SCF	OLYP[5]	PW91[5]	B3LYP-D3[5]
1.52	1.67	1.03	1.09	0.45

- SC-NEVPT2 confirms the singlet ground state prediction of DFT
- DFT energies significantly lower – OLYP and PW91 energies closest
- SC-NEVPT2 not far off from DMRG-SCF
    - dynamic correlation well covered in large (22,22) active space?

L. Freitag, S. Knecht, C. Angeli, M. Reiher, JCTC (2016) under review (arXiv:1608.02006)

[5] Hopmann et al., Inorg. Chem. 2015, 54, 7362

Dynamic Correlation through (short-range) DFT

Dynamic correlation through short-range DFT

Decomposition into active and inactive system

$$E_{\mathsf{CAS\text{-}CI}} = E_{\mathsf{I}} + E_{\mathsf{A}}$$

where

$$E_{\mathrm{I}} = \frac{1}{2}\sum_{ij}\left(h_{ij} + f^{\mathsf{I}}_{ij}\right)D^{\mathsf{I}}_{ij} + V_{\mathsf{nn}} = \sum_{i}\left(h_{ii} + f^{\mathsf{I}}_{ii}\right) + V_{\mathsf{nn}}$$

$$E_{\mathrm{A}} = \sum_{uv} f^{\mathsf{I}}_{uv} D^{\mathsf{A}}_{uv} + \frac{1}{2}\sum_{uvxy} g_{uvxy} P^{\mathrm{A}}_{uvxy}$$

with

$$f^{\mathsf{I}}_{pq} = h_{pq} + \sum_{k}\left(2g_{pqkk} - g_{pkqk}\right)$$

and

$$g_{pqrs} = \langle \phi_p(\boldsymbol{r}_1)\phi_r(\boldsymbol{r}_2)|\hat{g}(1,2)|\phi_q(\boldsymbol{r}_1)\phi_s(\boldsymbol{r}_2)\rangle$$

Dynamic correlation through short-range DFT

Introduce the range separation into the electron–electron interaction

$$\hat{g}(1,2) = \hat{g}^{\mu,\mathsf{lr}}(1,2) + \hat{g}^{\mu,\mathsf{sr}}(1,2)$$

with

$$\hat{g}^{\mu,\mathsf{lr}}(1,2) = \frac{\mathsf{erf}(\mu|\boldsymbol{r}_1 - \boldsymbol{r}_2|)}{|\boldsymbol{r}_1 - \boldsymbol{r}_2|}$$

$$\hat{g}^{\mu,\mathsf{sr}}(1,2) = \frac{1 - \mathsf{erf}(\mu|\boldsymbol{r}_1 - \boldsymbol{r}_2|)}{|\boldsymbol{r}_1 - \boldsymbol{r}_2|}$$

Then, the energy can be set up as

$$E^{\mathsf{srDFT}}_{\mathsf{CAS\text{-}CI}} = E^{\mathsf{lr}}_{\mathsf{I}} + E^{\mathsf{lr}}_{\mathsf{A}} + E^{\mathsf{sr}}_{\mathsf{H}}[\rho] + E^{\mathsf{sr}}_{\mathsf{xc}}[\rho]$$

Regularizing effect of srDFT on small CAS: Water

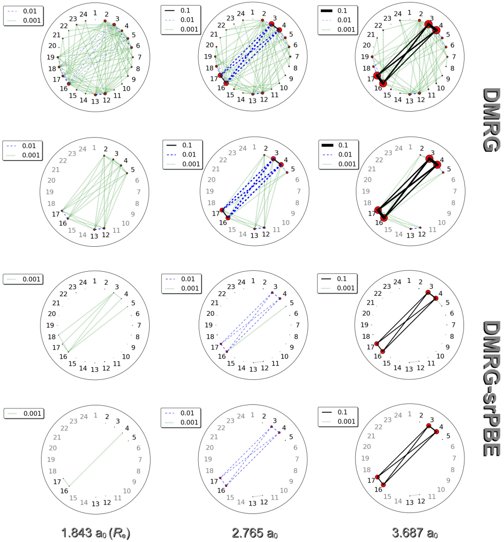

E. D. Hedegård, S. Knecht, J. S. Kielberg, H. J. A. Jensen, and M. Reiher, *J. Chem. Phys.* 142 **2015** 224108

DMRG–srDFT for the WCCR10 test set

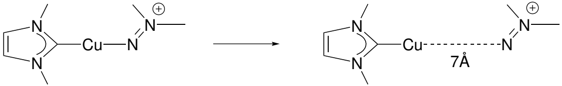

Calculated dissociation energies in kJ/mol

Method	D_e (kJ/mol)	D_0 (kJ/mol)
DMRG[2000](30,22)	173.5	165.1
DMRG[2000](20,18)	169.9	161.5
DMRG[2000](10,10)	132.8	124.3
DMRG[2000](30,22)-srPBE	225.1	216.6
DMRG[2000](20,18)-srPBE	227.9	219.4
DMRG[2000](10,10)-srPBE	216.5	208.0
PBE	240.2	231.8
PBE (full complex/def2-TZVP)	257.5	249.0
PBE (full complex/def2-QZVPP from WCCR10)	247.5	239.0
Exp. (from WCCR10)	226.7	218.2

E. D. Hedegård, S. Knecht, J. S. Kielberg, H. J. A. Jensen, and M. Reiher, *J. Chem. Phys.* 142 **2015** 224108;
WCCR10: T. Weymuth, E. P. A. Couzijn, P. Chen, M. Reiher, *J. Chem. Theory Comput.* 10 **2014** 3092

DMRG for solving the nuclear Schrödinger equation?

Ab initio calculation of vibrational energies

1. Expand the electronic energy in a set of coordinates *q* (internal, Cartesian, normal ...):

$$\begin{aligned} V(q) =& V_{\text{eq}} + \sum_i \left(\frac{\partial V}{\partial q_i}\right) + \frac{1}{2!}\sum_{i,j}\left(\frac{\partial^2 V}{\partial q_i \partial q_j}\right)_{\text{eq}} q_i q_j \\ & + \frac{1}{3!}\sum_{i,j,k}\left(\frac{\partial^3 V}{\partial q_i \partial q_j \partial q_k}\right)_{\text{eq}} q_i q_j q_k + \frac{1}{4!}\sum_{i,j,k,l}\left(\frac{\partial^4 V}{\partial q_i \partial q_j \partial q_k \partial q_l}\right)_{\text{eq}} q_i q_j q_k q_l + \ldots \end{aligned}$$

2. Solve the nuclear Schrödinger equation with this potential:

$$\hat{H}(V)\Psi_{\text{vib}} = E\Psi_{\text{vib}}$$

Calculation of vibrational energies

Calculation of the potential requires choice of:

- electronic structure method (cost vs. accuracy)
- coordinates
- fitting procedure

Approximate solution of the nuclear Schrödinger equation:

- harmonic or anharmonic calculation
- perturbative approaches (VPT2 …)
- variational approaches (VSCF, VCI ...)

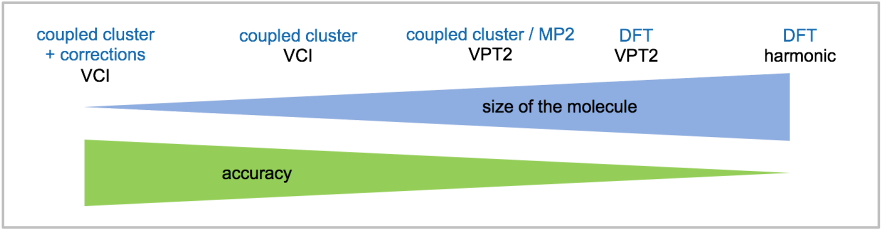

coupled cluster
+ corrections
VCI

coupled cluster
VCI

coupled cluster / MP2
VPT2

DFT
VPT2

DFT
harmonic

size of the molecule

accuracy

How to reduce the computational effort?

Exact diagonalization unfeasible for molecules with more than ~ 8-10 atoms.

⟶ different techniques to reduce the computational effort:

- basis pruning algorithms
  (Carrington…)
- contracted basis techniques
  (Handy, Carrington…)
- local mode approaches
  (Jacob, Reiher, Steele, Christiansen ...)
- reduced dimensionality schemes
  (Allen, Barone, Bloino ...)

- Tensor formats
  (Carrington, Oseledets)

⟶ Density Matrix Renormalization Group to optimize the vibrational wave function (vDMRG)

vDMRG – the wave function

Full configuration interaction wave function of the *k*-th vibrational state:

expansion coefficient

occupation number vector (ONV)

$$|\Psi_k\rangle = \sum_{\sigma_1,\ldots,\sigma'_L=0}^{1} C^{(k)}_{\sigma_1,\ldots,\sigma_{L'}} |\sigma_1,\ldots,\sigma_{L'}\rangle$$

L' vibrational basis functions

harmonic oscillator (HO) basis functions:
→ *L'* = $N_{\max}$ x *L*
($N_{\max}$ basis functions per mode *L*)

$$|\Psi_k\rangle = \sum_{\sigma_1,\ldots,\sigma_L=0}^{N_{\max}} C^{(k)}_{\sigma_1,\ldots,\sigma_L} |\sigma_1,\ldots,\sigma_L\rangle$$

Expressed as a matrix product state (MPS):

Tensor Train format of Rakhuba and Oseledets (*JCP* (**2016**), *145*, 124101) is equivalent to MPS!

maximum bond dimension

vector

vector

$$|\Psi_k\rangle = \sum_{\sigma_1,\ldots,\sigma_L}^{N_{\max}} \sum_{a_1,\ldots,a_{L-1}}^{[m]} M^{(k)\sigma_1}_{1,a_1} \underbrace{M^{(k)\sigma_2}_{a_1,a_2} \ldots}_{\text{matrices}} M^{(k)\sigma_L}_{a_{L-1},1} |\sigma_1,\ldots,\sigma_L\rangle$$

A. Baiardi, C.J. Stein, V. Barone, M. Reiher, *JCTC* (**2017**), *submitted*, arXiv: 1703.09313

vDMRG – the wave function

$$|\Psi_k\rangle = \sum_{\sigma_1,\ldots,\sigma_L}^{N_{\max}} \sum_{a_1,\ldots,a_{\text{L-1}}}^{[m]} \mathbf{M}^{(k)\sigma_1}_{1,a_1} \mathbf{M}^{(k)\sigma_2}_{a_1,a_2} \ldots \mathbf{M}^{(k)\sigma_L}_{a_{\text{L-1}},1} |\sigma_1,\ldots,\sigma_L\rangle$$

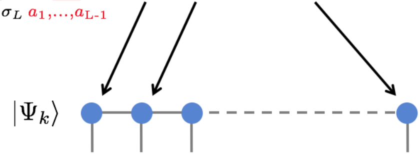

—●— : vibrational mode, *site*

m : maximum dimension of site matrix, *determines fraction of CI space recovered*

N_{max} : maximum quanta of excitation per mode, *size of local basis*
⟶ currently fixed for all modes; could be taken as mode-dependent variable

Characteristics of the MPS structure:

- **ordering** of the modes (sites) is important (better description of local correlations): faster convergence for strongly coupled modes next to another on the lattice

A. Baiardi, C.J. Stein, V. Barone, M. Reiher, *JCTC* (**2017**), *submitted*, arXiv: 1703.09313

vDMRG – Watson Hamiltonian

Watson Hamiltonian in normal coordinates with electronic potential *V*:

$$\hat{H}_{\text{vib}} = \frac{1}{2}\sum_{i=1}^{L} \omega_i \left(\hat{p}_i^2 + \hat{q}_i^2\right) + \frac{1}{6}\sum_{ijk=1}^{L} \Phi_{ijk}\hat{q}_i\hat{q}_j\hat{q}_k + \frac{1}{24}\sum_{ijkl=1}^{L} \Phi_{ijkl}\hat{q}_i\hat{q}_j\hat{q}_k\hat{q}_l + \frac{1}{24}\sum_{ijkl=1}^{L}\sum_{\tau}^{x,y,z} B^{\tau}\zeta_{ij}^{\tau}\zeta_{kl}^{\tau}\left(\frac{\omega_j\omega_l}{\omega_i\omega_k}\right)\hat{q}_i\hat{p}_j\hat{q}_k\hat{p}_l$$

$\hat{q}_i$ = position operator

$\hat{p}_i$ = momentum operator conjugate to $\hat{q}_i$

$\boldsymbol{\Phi}_{ijk}$ = third-order reduced force constant

$\boldsymbol{\Phi}_{ijkl}$ = fourth-order reduced force constant

B^{τ} = rotational constant

ζ_{ij}^{τ} = Coriolis coupling constant

- widely used Hamiltonian in many applications
- extension to higher orders is straightforward (currently up to 6th order implemented)

J.K.G. Watson, *Mol. Phys.* (**1968**), *15*, 479.

vDMRG – Watson Hamiltonian

For the DMRG algorithm, a second-quantized Hamiltonian is required

translate $\hat{q}_i = \frac{1}{\sqrt{2}}\left(\hat{b}_i^+ + \hat{b}_i\right)$ and $\hat{p}_i = \frac{1}{\sqrt{2}}\left(\hat{b}_i^+ - \hat{b}_i\right)$

with 2nd quantized creation and annihilation operators defined as:

$$\hat{b}_i^+|\sigma_1, ..., \sigma_i, ..., \sigma_L\rangle = \sqrt{\sigma_i + 1}|\sigma_1, ..., \sigma_i + 1, ..., \sigma_L\rangle\,,$$

$$\hat{b}_i|\sigma_1, ..., \sigma_i, ..., \sigma_L\rangle = \begin{cases} \sqrt{\sigma_i}|\sigma_1, ..., \sigma_i - 1, ..., \sigma_L\rangle, \text{ if } \sigma_i > 0 \\ 0, \text{ if } \sigma_i = 0\,. \end{cases}$$

Final 2nd quantized Watson Hamiltonian:

$$\hat{H}_{\text{vib}} = \sum_{i=1}^{L} \omega_i \left(\hat{b}_i^+\hat{b}_i + \frac{1}{2}\right) + \frac{1}{12\sqrt{2}} \sum_{ijk=1}^{L} \mathbf{\Phi}_{ijk} \left(\hat{b}_i^+ + \hat{b}_i\right)\left(\hat{b}_j^+ + \hat{b}_j\right)\left(\hat{b}_k^+ + \hat{b}_k\right)$$
$$+ \frac{1}{96} \sum_{ijkl=1}^{L} \mathbf{\Phi}_{ijkl} \left(\hat{b}_i^+ + \hat{b}_i\right)\left(\hat{b}_j^+ + \hat{b}_j\right)\left(\hat{b}_k^+ + \hat{b}_k\right)\left(\hat{b}_l^+ + \hat{b}_l\right)$$
$$+ \frac{1}{96} \sum_{ijkl=1}^{L} \sum_{\tau}^{x,y,z} B^{\tau} \zeta_{ij}^{\tau} \zeta_{kl}^{\tau} \left(\frac{\omega_j\omega_l}{\omega_i\omega_k}\right) \left(\hat{b}_i^+ + \hat{b}_i\right)\left(\hat{b}_j^+ - \hat{b}_j\right)\left(\hat{b}_k^+ + \hat{b}_k\right)\left(\hat{b}_l^+ - \hat{b}_l\right)$$

S. Hirata, M. R. Hermes, *JCP* (**2014**), *141*, 184111.

vDMRG – Watson Hamiltonian in MPO format

Express this Hamiltonian in Matrix Product Operator (MPO) format:

$$\hat{W} = \sum_{\sigma\sigma'} \sum_{b_1,\ldots,b_{L-1}} \overset{\overset{\text{vector}}{\downarrow}}{W^{\sigma_1,\sigma_1'}_{1b_1}} \underbrace{\ldots W^{\sigma_i,\sigma_i'}_{b_{i-1}b_i} \ldots}_{\text{matrices}} \overset{\overset{\text{vector}}{\downarrow}}{W^{\sigma_L,\sigma_L'}_{b_{L-1}1}} \underbrace{|\sigma\rangle\langle\sigma'|}_{\text{ONVs}}$$

symbolic representation

As an example, we write the harmonic term on site *i* in MPO form (not dependent on *m*):

$$\hat{H}_{\text{harm.}}(i) = \omega_i \left(\hat{b}_i^+ \hat{b}_i + \frac{1}{2} \right) \longrightarrow \hat{W}_{\text{harm.}}(i) = \omega_i \cdot \hat{I}_1 \overset{\overset{\text{unit matrices of max. dimension } N_{\text{max}}}{\downarrow}}{\otimes \cdots \otimes} \underbrace{\hat{b}_i^+ \cdot \hat{b}_i}_{\text{matrix representation of elementary operators}} \otimes \cdots \otimes \hat{I}_L$$

- extremely sparse matrix!

  ⟶ sparse, iterative eigensolvers (Jacobi-Davidson)
  iterative procedure with decimation steps

A. Baiardi, C.J. Stein, V. Barone, M. Reiher, *JCTC* (**2017**), *submitted*, arXiv: 1703.09313

Proof of concept – ClO$_2$

Parameters of vDMRG

N_{max} : size of local basis	increases with anharmonicity
m: max. dimension of site matrices	increases with anharmonic mode-coupling
number of sweeps	increases with anharmonicity

→ 20 sweeps ensured convergence for all states

$X\,^2B_1$ ground state

- internally contracted MRCI+Q on CAS (13,9) active space[1]
- adjusted cc-pVQZ basis set
- quartic fit in internal coordinates

→

- direct tensor transformation to normal coordinates[2]
- up to sextic terms included

[1] K. A. Peterson, *JCP* (**1998**), *109*, 8864.
[2] M. Sibaev, D. L. Crittenden, *J. Comput. Chem.* (**2015**), *36*, 2200.

Proof of concept – ClO_2

		N_{max} = 10			N_{max} = 12	
assignment	Ref.[1]	m = 2	m = 5	m = 10	m = 5	m = 10
ZPE		1264.5	1264.5	1264.5	1264.5	1264.5
ν_2	449.9	449.5	449.5	449.5	449.5	449.5
ν_1	940.7	940.7	940.7	940.7	940.7	940.5
ν_3	1105.5	1105.2	1105.2	1105.2	1105.2	1105.2
$2\nu_1 + \nu_2$	2313.8	2318.4	2313.5	2313.6	2313.6	2313.7
$2\nu_1 + \nu_3$	2943.2	2947.9	2943.8	2943.2	2943.5	2943.7

Energies in cm^{-1}; [1] K. A. Peterson, *JCP* (**1998**), *109*, 8864.

- very low bond dimension *m* is sufficient to converge energies
- results are effectively converged w.r.t. basis set size for N_{max} = 10
- slightly larger *m* is required for higher excited states (here: combination bands)

A. Baiardi, C.J. Stein, V. Barone, M. Reiher, *JCTC* (**2017**), *submitted*, arXiv: 1703.09313

Parameter dependence – CH_3CN

- full quartic force-field from CCSD(T)/cc-pVTZ//B3LYP/cc-pVTZ
  (D. Begue, P. Carbonnière, C. Pouchan, *JPCA* (**2005**), *109*, 4611.)
- became a classic benchmark for several new variational methods
  (A. Leclerc, P.S. Thomas, T. Carrington, *Mol. Phys.* (**2016**) doi:10.1080/00268976.2016.1249980 M. Rakhuba, I. Oseledets, *JCP* (**2016**), *145*, 124101. G. Avila, T. Carrington, *JCP* (**2011**), *134*, 054126. A. Leclerc, T. Carrington, *JCP* (**2014**), *140*, 174111. A. Leclerc, T. Carrington, *CPL* (**2016**), *644*, 183.)

only force constants > 7 cm^{-1} were reported by D. Begue *et al*.

⟶ study parameter dependence of energy convergence

---

convergence w.r.t. number of sweeps is simple to monitor

↓

criterion: $E_{\text{curr. sweep}} - E_{\text{curr. sweep - 10}} \leq 0.001 \text{ cm}^{-1}$

↓

15 – 250 sweeps depending on state

A. Baiardi, C.J. Stein, V. Barone, M. Reiher, *JCTC* (**2017**), *submitted*, arXiv: 1703.09313

Parameter dependence – CH_3CN

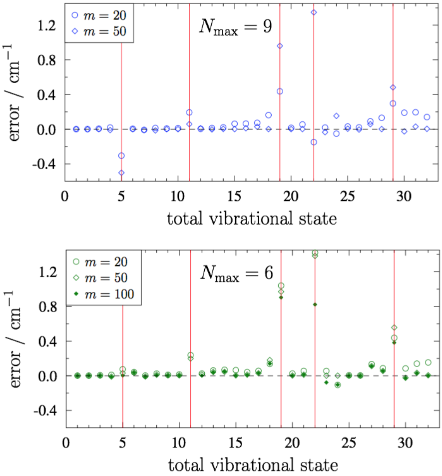

- reference calculation with vDMRG: $N_{\max}$ = 9, m = 100
- deviations in **most cases below 0.2 cm^{-1}**
- larger errors for strongly interacting states
- *m* = 20 takes **only 15 %** of the computational time of *m* = 100

→ *m* = 20 sufficient for sub cm^{-1} accuracy

A. Baiardi, C.J. Stein, V. Barone, M. Reiher, *JCTC* (**2017**), *submitted*, arXiv: 1703.09313

Higher-order expansion of the force field – C_2H_4

electronic ground state

- quartic CCSD(T) / pVQZ potential energy surface in internal coordinates
  T. Delahaye, A. Nikitin, M. Rey, P. Szalay, V.G. Tyuterev, *JCP* (**2014**), *141*, 104301.
- converted to a sextic potential in normal coordinates by a direct tensor transformation (nonlinear transformation) A. Hoy, I. Mills; G. Strey, *Mol. Phys.* (**1972**), *24*, 1265.
- calculations with and without Coriolis terms in the Hamiltonian

---

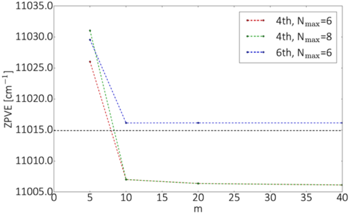

- *m* = 10 gives converged results (within 1cm^{-1})
- 6th order expansion is necessary
- N_{max} = 6 sufficient for low lying states

A. Baiardi, C.J. Stein, V. Barone, M. Reiher, *JCTC* (**2017**), *submitted*, arXiv: 1703.09313.

Higher-order expansion of the force field – C_2H_4

		no Coriolis		Coriolis	no Coriolis	
mode	assignment	m = 10	m = 20	m = 10	Ref. [1]	Exp. [2]
ZPVE		11016.14	11016.15	11021.39	11014.91	
2	ν_8	933.48	933.47	942.26	934.29	939.86
4	ν_4	1018.26	1018.26	1026.64	1024.94	1025.58
5	ν_6	1227.08	1227.05	1229.68	1224.96	1225.41
6	ν_3	1343.46	1343.46	1344.25	1342.96	1343.31
11	$\nu_7 + \nu_{10}$	1787.02	1786.99	1781.17	1778.34	1781.01

Energies in cm^{-1}. N_{max} is set to 6 and 10 sweeps were run in all calculations.

- again, small value of *m* sufficient for converged results
- vDMRG (approximate VCI) calculations feasible for medium size systems including terms higher than quartic
- inclusion of Coriolis effects (last term in Watson Hamiltonian) in general improves the results

A. Baiardi, C.J. Stein, V. Barone, M. Reiher, *JCTC* (**2017**), *submitted*, arXiv: 1703.09313
[1] T. Delahaye, A. Nikitin, M. Rey, P. Szalay, V.G. Tyuterev, *JCP* (**2014**), *141*, 104301.
[2] R. Georges, M. Bach, M. Herman, *Mol. Phys.* (**1999**), *97*, 279.

A large molecule – the SarGly$^+$ dipeptide

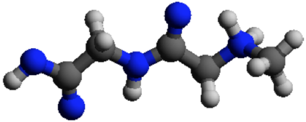

- B3LYP/6-311+G(d,p) quartic force-field
- neglect quartic force constants with four different indices and those < 1cm^{-1}
- harmonic treatment for all modes below 900 cm^{-1}

- focus on **fingerprint region** (~ 900 – 1700 cm^{-1})
- **35 modes** treated fully variationally
- total of **3964 terms in the Hamiltonian** (1648 for sextic potential in C_2H_4)

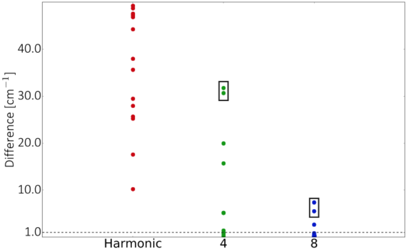

very fast sweep convergence
(in black rectangle: resonant states)

A. Baiardi, C.J. Stein, V. Barone, M. Reiher, *JCTC* (**2017**), *submitted*, arXiv: 1703.09313

A large molecule – the SarGly⁺ dipeptide

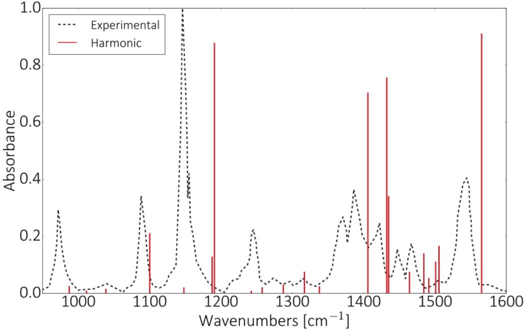

A large molecule – the SarGly⁺ dipeptide

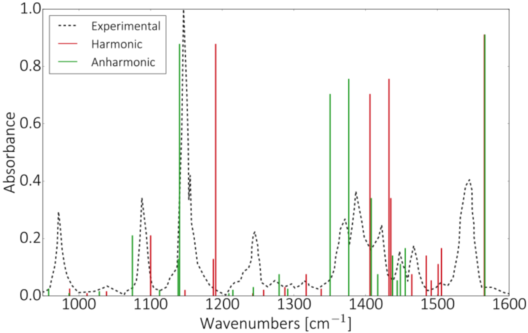

- harmonic intensities
- approximately 5h per total vibrational state in current implementation
- red shift and better agreement with experimental spectrum

A. Baiardi, C.J. Stein, V. Barone, M. Reiher, *JCTC* (**2017**), *submitted*, arXiv: 1703.09313

Acknowledgements

- **Current Group Members:**
  Leon Freitag, Tamara Husch, Stefan Knecht, Arseny Kovyrshin, Adrian Mühlbach, Andrea Muolo, Jonny Proppe, Gregor Simm, Jan-Grimo Sobez, Christopher Stein, Alain Vaucher, Vera von Burg

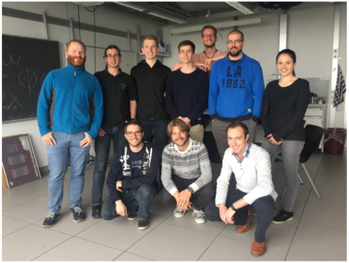

Thank you for your kind attention!

- **Collaborators on vDMRG:**
  Alberto Baiardi (Pisa)
  Prof. Vincenzo Barone (Pisa)

- **Financial Support:**
  ETH, SNF, FCI, FWF

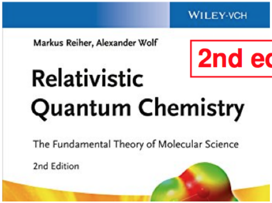

WILEY-VCH

Markus Reiher, Alexander Wolf

Relativistic Quantum Chemistry

The Fundamental Theory of Molecular Science

2nd Edition

2nd edition